NOVEL FABRICATION OF FLEXIBLE ELECTRONICS BY TRANSFER PRINTING PROCESS

A Thesis

Presented to

The Faculty of the Department of Mechanical Engineering

University of Houston

In Partial Fulfillment

of the Requirements for the Degree

Master of Science

In Mechanical Engineering

by

Song Chen

December 2016

NOVEL FABRICATION OF FLEXIBLE ELECTRONICS

BY TRANSFER PRINTING PROCESS

Song Chen

Approved:

Chair of the committee
Cunjiang Yu, Assistant Professor,
Mechanical Engineering

Committee Members:

Liu Dong, Assistant Professor,
Mechanical Engineering

Jiming Bao, Associate Professor,
Mechanical Engineering

Suresh K. Khator, Associate Dean,
Cullen College of Engineering

Pradeep Sharma
Chair of Dept in Mechanical Engineering

Acknowledgments

I would like to convey my gratitude to my supervisors: Dr. Cunjiang Yu and Dr. Gangbing Song for their consistent instruction and guidance to help me develop skill sets on micro-fabrication and make sense of modern control theory. I was impressed by their diligence, rigorousness, erudition and motivation to make efforts to make breakthrough on research. And I would like to express appreciation for their assistance on my experiment, hardly any result come out quickly without their collaboration. I wish they become productive in their following research career.

I would like to thank Dr. Dong Liu for the ‘green-light’ that he has given to us to use facilities in his lab, some experiments could be conducted by courtesy of his instructions. I admire Dr. Jiming Bao’s knowledge and experience on nanofabrication, his course helps me build up sense and understanding. Also, I thank staff members including Ms. April Blout, Joana Tan, Smith Cecily and Ms. Tracy Ann Pringer in Mechanical Engineering Department for their administrative contribution to students and Mr. Jerry Clifton for his technical support. Finally, I am grateful for all the kind people I have ever met and worked with in UH.

NOVEL FABRICATION OF FLEXIBLE ELECTRONICS

BY TRANSFER PRINTING PROCESS

An abstract

of a

thesis

Presented to

The Faculty of the Department of Mechanical Engineering

University of Houston

In Partial Fulfillment

of the Requirements for the Degree

Master of Science

In Mechanical Engineering

By

Song Chen

December 2016

Abstract

Stretchable electronics, represents a class of novel electronic devices fabricated on flexible and bendable substrate, has been researched widely due to its applications cover from epidermal electronics (eSkin), curvillinear display, bio-integrated electronics to photovoltaics. Generally, the electronics can be formed by printing devices onto the flexible substrate (donor) by rubber 'stamp', for example, the transistors, diodes, and logic circuits can be picked up after peeling back the elastormeric prepolymer (Polydimethylsiloxane) (PDMS) laminated on the surface of wafer and then contact the 'inked' stamp onto target substrate (receiver), peeling off the PDMS will leave the 'ink' on the flexible substrate. The 'pick-up' process depends strongly on the speed of lamination because the separation energy for elastomer-microstructure interface is related to speed while the one for microstructure-substrate is independent. The yield of the transfer printed is reported as high as 100% without losing function. Besides of solid rubber like PDMS, tape can also be used in the transfer printing process and it's been reported that this has been implemented to fabricate RF stretchable electronics with liquid metal alloy. In this thesis, a novel balloon transfer printing method (a polymer-coated balloon serves as 'stamp') is presented that is useful to fabricate curvillinear electronics, exemplify a smart contact lens similar to Google's new roll-out. Besides, a tape transfer printing process with high fidelity facilitated by chemically induced adhesive strength

modulation is presented. Silicon and metal mesh devices transfer printed by tape on flexible substrate is demonstrated and its functionality is verified by testing. Finally, the corporate project with NASA Johnson Space Center aims to develop a skin mountable patch for exercise monitoring is introduced as well as its related progress.

Table of Contents

Acknowledgments.....iv

Abstract.....vi

Table of Contents.....viii

List of Figures.....x

1. Introduction.....1

2. Exploration of high fidelity transfer printing based on solution-involved adhesive strength modulation

2.1 Introduction.....11

2.2 Tape transfer printing.....12

3. Exploration of fabrication by balloon transfer printing (BTP)

3.1 Introduction.....20

3.2 Smart Contact Lens.....20

3.3 Balloon Transfer Printing.....27

4. Exploration of eSkin technology

4.1 Wearable electronics.....31

4.2 Skin mountable electronics.....32

4.3 Skin stamps for coupled multi parametric physiological sensing and environmental monitoring.....35

4.3.1 Physiological monitoring application for astronauts.....36

4.3.2 Ultra-thin skin mountable stamps.....38

4.3.2.1 Arduino Uno.....43

4.3.2.2 Sensors 44

4.3.2.3 Result.....47

5. Conclusion.....53

References.....55

List of Figures

Fig. 1 Microcontact printing.....2

Fig. 2 Microcontact printing by glass cylinder.....2

Fig. 3 Organic complemetary inverter printed by using cylindrical stamp.....2

Fig. 4 Smart pixels and I-V curve of LED.....3

Fig. 5 Nanotransfer printing (nTP) process.....4

Fig. 6 Fabrication of GaAs transistor by nTP process and comparison of I-V curve for 2-termial junction fabricated by control, evaporated and nTP.....5

Fig. 7 Transfer printed nanowires and microwires on PET substrate and I-V curve under different radius of bend.....7

Fig. 8 Transfer print Single-Wall Carbon Nanotube (SWNT) film synthesized by controlled flocculation process.....8

Fig. 9 Transfer print different patterns (dots, lines and cross patterns of lines) of SWNT onto APTS-treated SiO2/Si and PMMA on Mylar.....9

Fig. 10 Process of transfer printing.....10

Fig. 11 Silicon array (a) and photodiode array (b) transfer printed onto non-planar substrate (c) photodiode on glass cylinder under microscope.....10

Fig. 12 Improve the yield of transfer printing by changing amount of pre-load.....12

Fig. 13 Tape transfer printing process.....13

Fig. 14 180° peel test and solvent wetting on substrate test.....15

Fig. 15 Tape transfer printing of photodiode array onto Polyimide film.....17

Fig. 16 Transfer printing of EMG sensor onto EcoFLEX patch.....18

Fig. 17 Transfer printing of silicon dot array onto curvilinear shape tube.....19

Fig. 18 Balloon transfer printing (BTP) process.....27

Fig. 19 Transfer printing of serpentine metal mesh and antenna.....30

Fig. 20 Google Co.'s Smart Contact Lens for glucose monitoring.....32

Fig. 21 Capacitive epidermic sensor.....34

Fig. 22 Electrocardiograms (ECGs) signal and measurement on chest, forearm and near left and right eye.....34

Fig. 23 Electromyograms (EMG) signal measured by capacitive sensor on forearm.35

Fig. 24 Crew Physiologic Observation Device (CPOD).....37

Fig. 25 IZO devices for physiological monitoring.....39

Fig. 26 Mask design of IZO devices.....40

Fig. 27 Microfludic assemblies and its deformation.....41

Fig. 28 Skin patch on forearm for electrophysiological monitoring.....42

Fig. 29 Skin mountable patch.....43

Fig. 30 Thermistor and connection to Arduino Uno.....45

Fig. 31 Skin mountable patch embeds temperature and humidity sensors.....47

Fig. 32 Humidity in environment and on skin surface.....48

Fig. 33 Temperature in environment and on skin surface.....49

Fig. 34 Skin mountable patch and Arduino Uno.....50

Fig. 35 Real-time acquisition and display of data from sensors.....50

Chapter 1

Introduction

Transfer printing technique has been widely used to fabricate electronics especially flexible electronics in the past decade. Initially, to fabricate flexible organic semiconductor, a so-called microcontact printing (uCP) technique that uses high resolution stamps fabricated with elastomeric elements can transfer the 'ink' to substrates has been reported [1, 2]. Figure 1 shows the fabrication of such elastomer stamp, to this end, a 'master' structure with feature size of 20nm fabricated by conventional lithography is required, then cast and cure elastomer onto the structure and peel it off like it is demonstrated in the Figure 1. The stamps can also be of cylindrical shape for the purpose of increasing the area of the printing, such stamp is fabricated by bonding PDMS onto a glass roller after exposure to oxygen plasma, as Figure 2 shows. In [3], the golden source/drain electrodes of organic complementary inverter circuit can be printed by using cylindrical stamp, the circuit and its transfer characteristics is shown in Figure 3. Besides, such non-photolithographical fabrication can be used to fabricate smart pixels as reported (Figure 4), which is composed of organic thin-film transistors (TFT's) and light emitting diode on the flexible substrate, the performance is equal to that of devices fabricated by conventional photolithographic process.

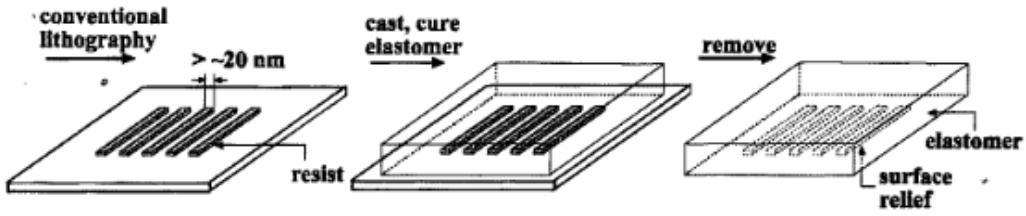

Fig. 1 Microcontact printing

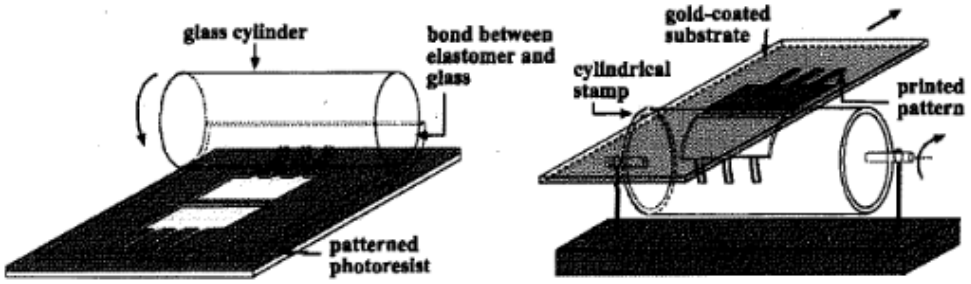

Fig. 2 Microcontact printing by glass cylinder

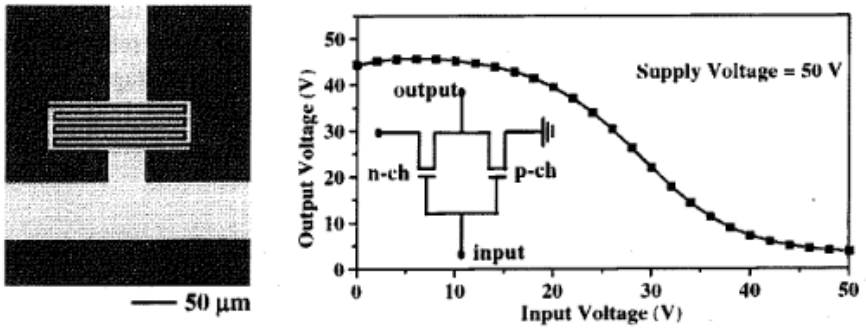

Fig. 3 Organic complemetary inverter printed by using cylindrical stamp

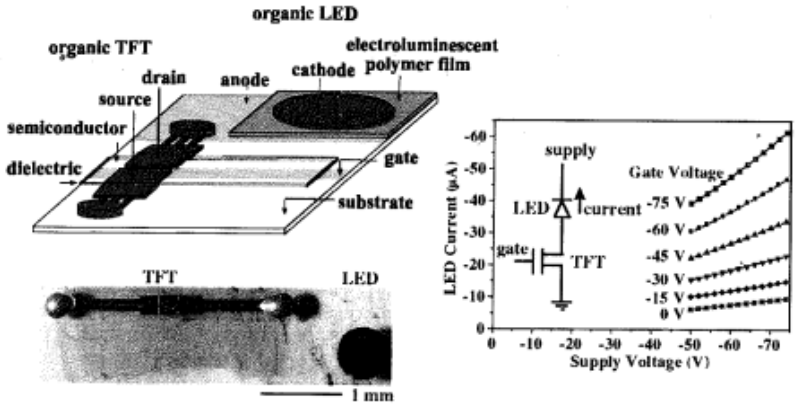

Fig. 4 Smart pixels and I-V curve of LED

However, the uCP is limited by its resolution in some application, mentioned less than 1um in the literature [4, 5, 6]. Yueh-Lin Loo *et al,* has presented a nanotransfer printing (nTP) whose resolution can reach nanometer level [7]. The procedure is similar to the uCP while starting with fabrication of high resolution stamps. The stamps can be either elastomeric like PDMS or rigid substrate, GaAs [8], whose features are defined by electron beam lithography. Such technique can transfer metal patterns onto conformal plastic and rigid substrateas (silicon), the printing procesure is shown in Figure. 5. The relief on the stamp is about 0.2-10um, and the lateral dimensions of features are between 0.05 and 100um. Both of the substrate and metal-coated stamp are oxidized by plasma before contact. Separating the stamp and substrate results in the completion of the transfer of pattern. The nTP process has already been used to fabricate the electrodes of organic molecular devices, and it has demonstrated superiority to other approaches like nanoscale junctions, mercury

droplets, lift-off float-on Au pads, and scanning probe tip electrodes on yield improvement (sometimes the electrodes across the molecules tend to become electrically shorted between contacts), Figure 6 shows a simple schematic of fabrication. The curve in Figure 6 shows a comparison of current level *vs* voltage curves for 2-terminal devices fabricated by control, evaporated, and nTP, the current level of junctions fabricated by nTP is 5 orders of magnitude lower than the others, more interestingly, there's no direct contact between gold and substrate (GaAs) was found and electrical transport exists in the solution deposited 1,8-octanedithiol molecular layer, which is different from the evaporated junctions where electrical transport is dominated by Ohmic contact.

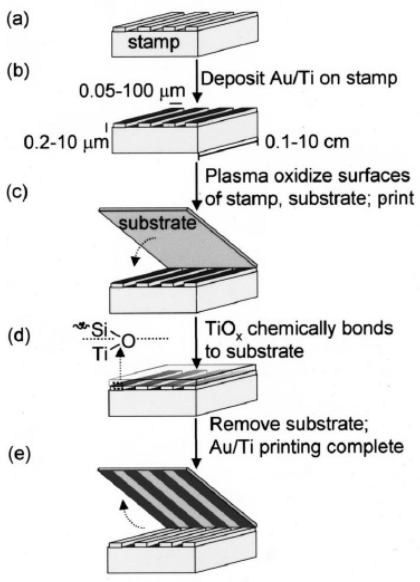

Fig. 5 Nanotransfer printing (nTP) process

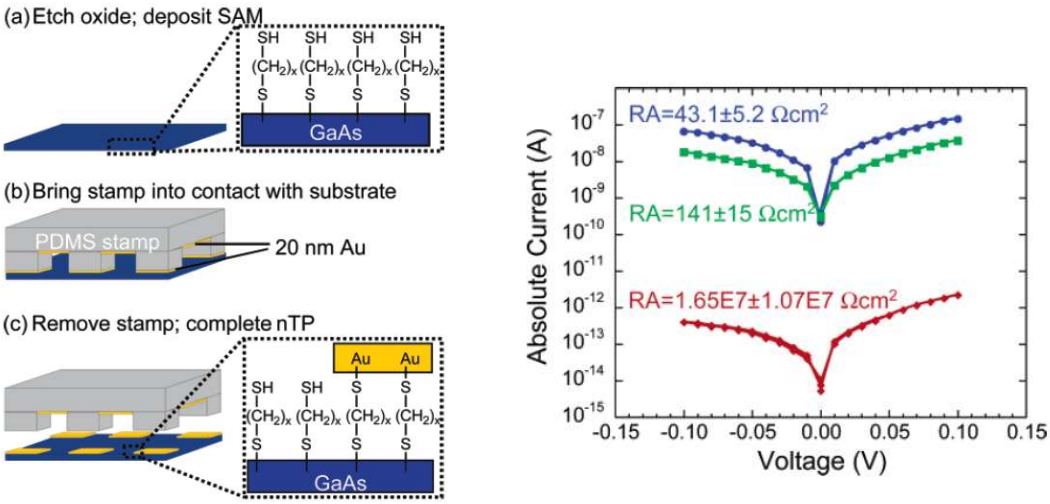

Fig. 6 Fabrication of GaAs transistor by nTP process and comparison of I-V curve for 2-termial junction fabricated by control, evaporated and nTP

Top down fabrication is prevalent in semiconductor industry, it is a subtractive process that etches the bulk through microstructure in wet or dry manner. It is meaningful to combine the top town fabrication with transfer printing to realize high performance macroelectronics. It has been reported transferring of GaAs nanowires and microwires onto PET plastic sheet without losing the orientation between wires [9]. The yield is as high as 100% and it displays a excellent mechanical performance. The electrical properties is measured on the condition of different bend radius as it is shown in the Figure 7 (b), and on the condition of release after bent to different radius Figure 7 (c). Such process is based on dry transfer printing as opposed to solution based wet transfer printing. Some promising materials like Single-Walled Carbon Nanotube (SWNT) films has been successfully transfer printed after

deposition from aqueous solution [10, 11]. However, deposition sometimes suffers from low coverage and is dependent on repeated depositions for dense SWNT film. M. A. Meitl *et al* has proposed a controlled flocculation (cF) process to deposit SWNT onto different substrates with a wide range of surface coverage [12]. The PDMS stamp can be 'inked' with SWNT film and used to transfer print the pattern onto the receiver substrate (Figure 8). The SEM photos of transfer printed patterns demonstrate high quality SWNT film on the target substrate (Figure 9 (a) Dots printed onto APTS-treated SiO2/Si (b) Lines deposited onto PMMA on Mylar (c) Cross-pattern of lines produced by two-step printing onto APTS-treated SiO2/Si (e) printed lines (light) on capillary tube (dark) with outer diameter 500 um). Worth a mention, as one of novel electronic materials, solution-cast SWNTs carry poor electrical properties and won't be earmarked for consumer electronics applications, but chemical vapor deposition (CVD) synthesized SWNTs can overcome this and be dry-printed onto flexible plastic substrate in order to form thin film transistors (TFTs) [13, 14].

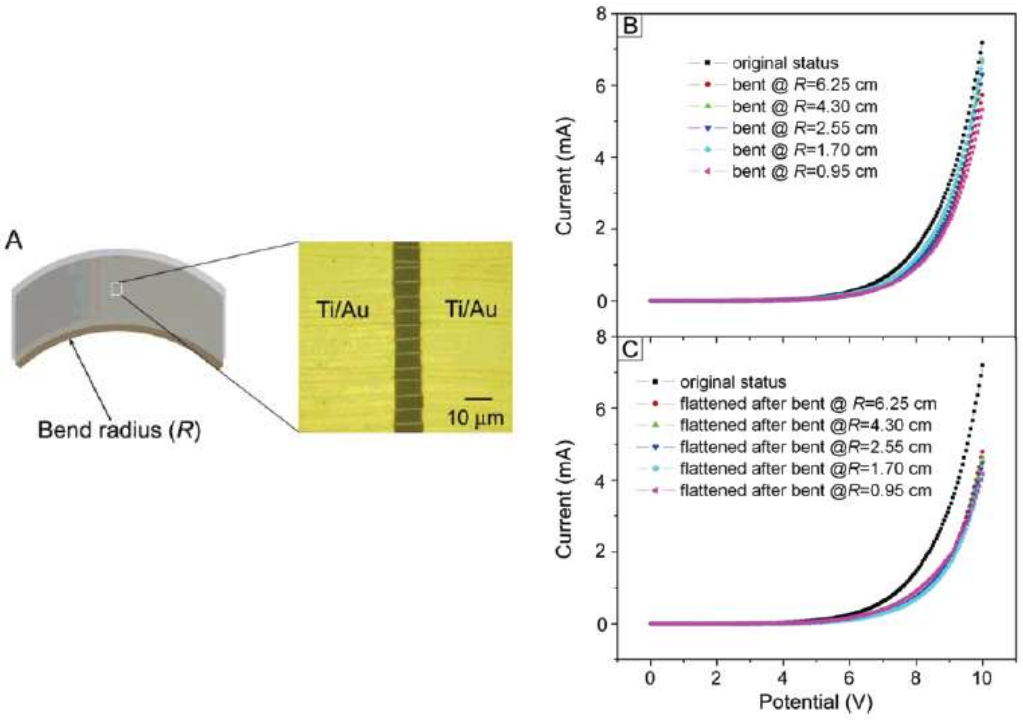

Fig. 7 Transfer printed nanowires and microwires on PET substrate and I-V curve under different radius of bend

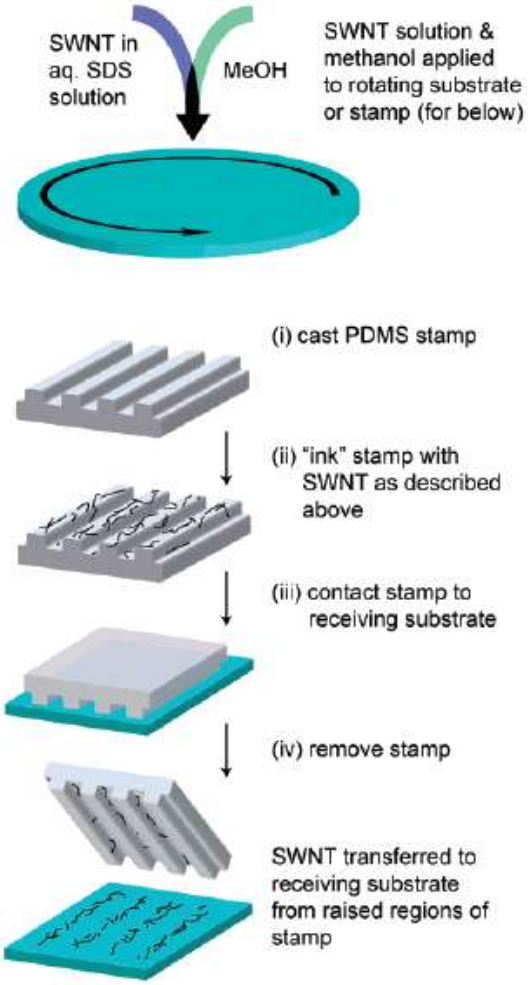

Fig. 8 Transfer print Single-Wall Carbon Nanotube (SWNT) film synthesized by controlled flocculation process

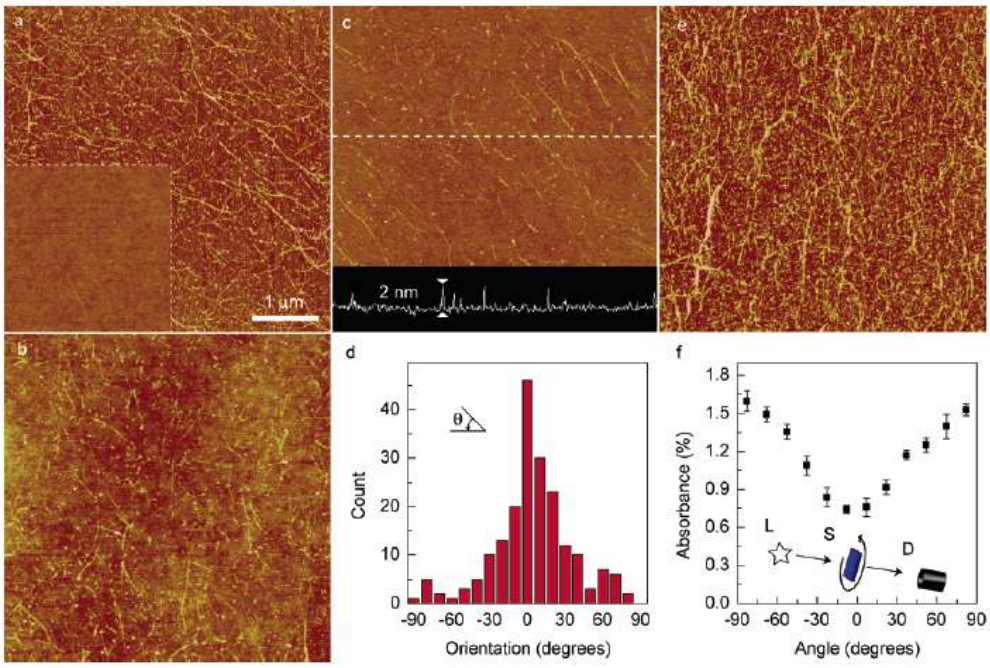

Fig. 9 Transfer print different patterns (dots, lines and cross patterns of lines) of SWNT onto APTS-treated SiO2/Si and PMMA on Mylar

Microcontact printing, nanoimprint and soft-photolithography has been considered as capable technology for patterning small feature size in the fabrication of electronic device and electronic material [15]. But they are not good candidate for heterogenerous integration of disparate classes of individual functional devices into system. Transfer printing provides a route for transferring, assembling and integrating the microstructured devices onto flexible macroelectronics system. Figure 10 shows the whole process of transfer printing [16] and Figure 11 shows the silicon dots array (a) and silicon photodiode (c) printed on the non-planar glass substrate.

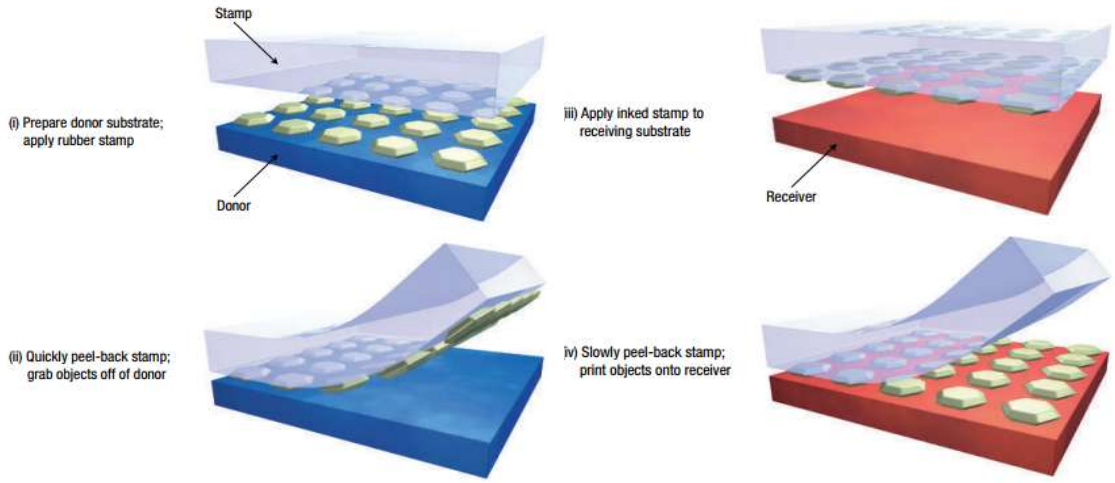

Fig. 10 Process of transfer printing

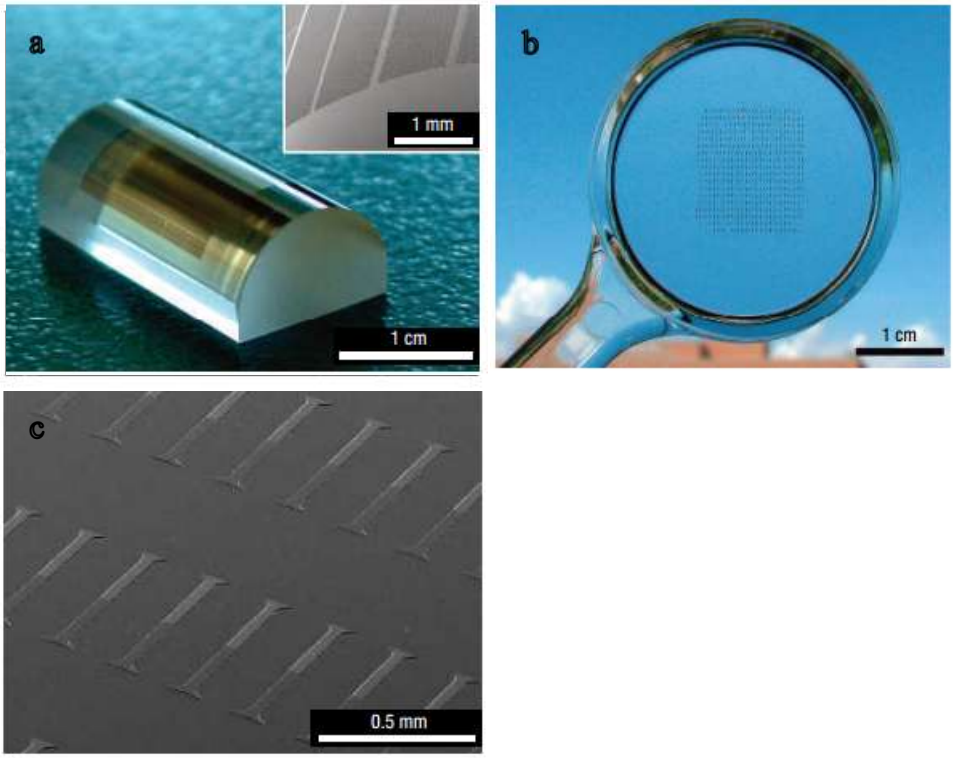

Fig. 11 Silicon array (a) and photodiode array (b) transfer printed onto non-planar substrate (c) photodiode on glass cylinder under microscope

Chapter 2

Exploration of high fidelity transfer printing based on solution-involved adhesive strength modulation

2.1 Introduction

Yield is most focused to evaluate the performance of transfer printing process, some high yield (>99%) transfer printing has been reported with regard to kinetic approaches that use viscoelasitic stamps for retrieval and delivery. The ability to switch from strong to weak adhesion is critical to achieve high yield. Shear-offset has been tried to be applied during delamination to increase yield [17], or change different preload on the stamp while retract it quickly and slowly to complete the transfer printing [18], the process is illustrated in Figure 12, different amount of preload is applied on initial contact with the target substrates. It is reported that enhancement of yield is facilitated by etching-assisted transfer printing (ETP) for construction of flexible organic nanowires devices [19]. The PMMA/electrodes films can be released in the solution to etch away the sacrificial metal layer and combined with target substrate when the substrate was lifted up in the deionized water bath. In this chapter, a high fidelity tape transfer printing (TTP) process based on solution-involved adhesive strength modulation will be proposed, and an array of target devices and materials before and after transfer printing will be demonstrated.

High fidelity (>99%) is realized on the target flexible substrate with retention of devices' function. It is helpful to the fabrication of sensors, display devices and other heterogenerous devices in the future.

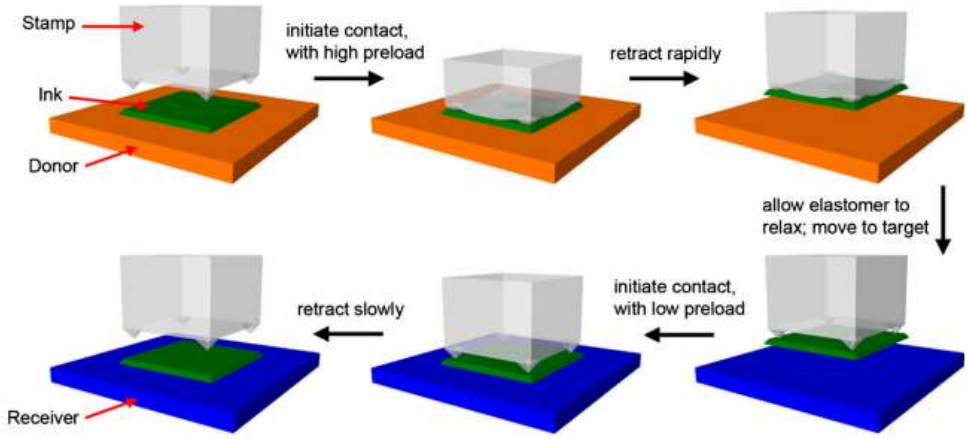

Fig. 12 Improve the yield of transfer printing by changing amount of pre-load

2.2 Tape transfer printing

Tape transfer printing has ever been used in fabricating liquid-alloy-based microfluidic stretchable electronics integrated with wireless communication capability [20]. The liquid alloy antenna was transfer printed by adhesive tape and hybrid integrated with ultra-high frequency (UHF) RFID chip to form frequency identification tag (RFID). Also, tape transfer printing technology has been used to fabricate flexible nanowires electronics. A thermal release tape serves as supporter of the devices and attached onto the top of the flexible target substrate.

After removal of silicon substrate with assistance of water, the thermal release tape is heated at 90℃for 5-6s and peeled off, only nanowire device is left on the target substrate.

Here a novel tape transfer printing process is proposed, details are shown in Figure 13.

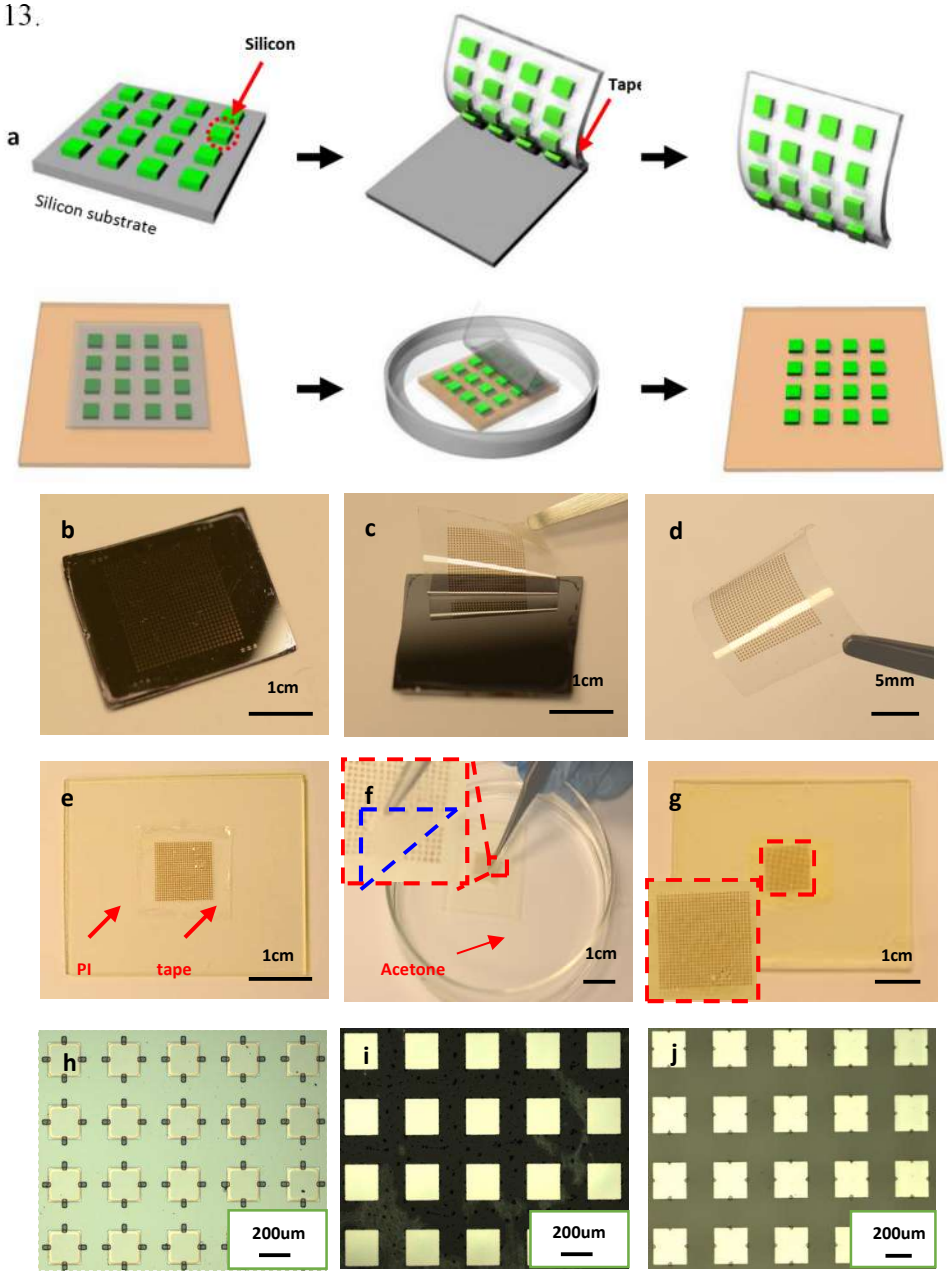

Fig. 13 Tape transfer printing process

Figure 13 (a) shows the schematic transfer printing process. (b)-(g) show the whole process of transfer printing silicon dots array. The silicon dots array was patterned by photolithography and reactive ion etching (RIE) on SOI wafer with 1.25um thick single crystal silicon. After undercut etching in buffer oxide etchant (BOE), anchors were patterned by photolithography to hold the silicon dots in the hydrofluoric acid HF (concentrated, 49%) etching process for SiO_2 layer removal. Eventually, the silicon dots array can be transferred onto the polyimide substrate coated on the glass, high yield is achieved (>99%). The transfer process is implemented in acetone solvent (f) because the adhesion strength of the tape will be reduced significantly with existence of acetone on the interface. A tape adhesive strength modulation test was conducted [21]. Refer to Figure 14 (a), it shows 180° peel test result of 3M 3850 tape before and after a squirt of acetone. Evident change occurs when acetone is introduced. In Figure 14 (c)-(e) display the wetting of the acetone on different substrates include tape liner, adhesive tape and glass. The acetone droplet starts spreading on the surface of adhesive tape but keep dewetting on the tape liner. Besides, different solvents' wetting has been tested to demonstrate acetone is a good fit for tape transfer printing, as Figure 14 (j) lists five kinds of solvents and four kinds of substrates involved in the wetting test.

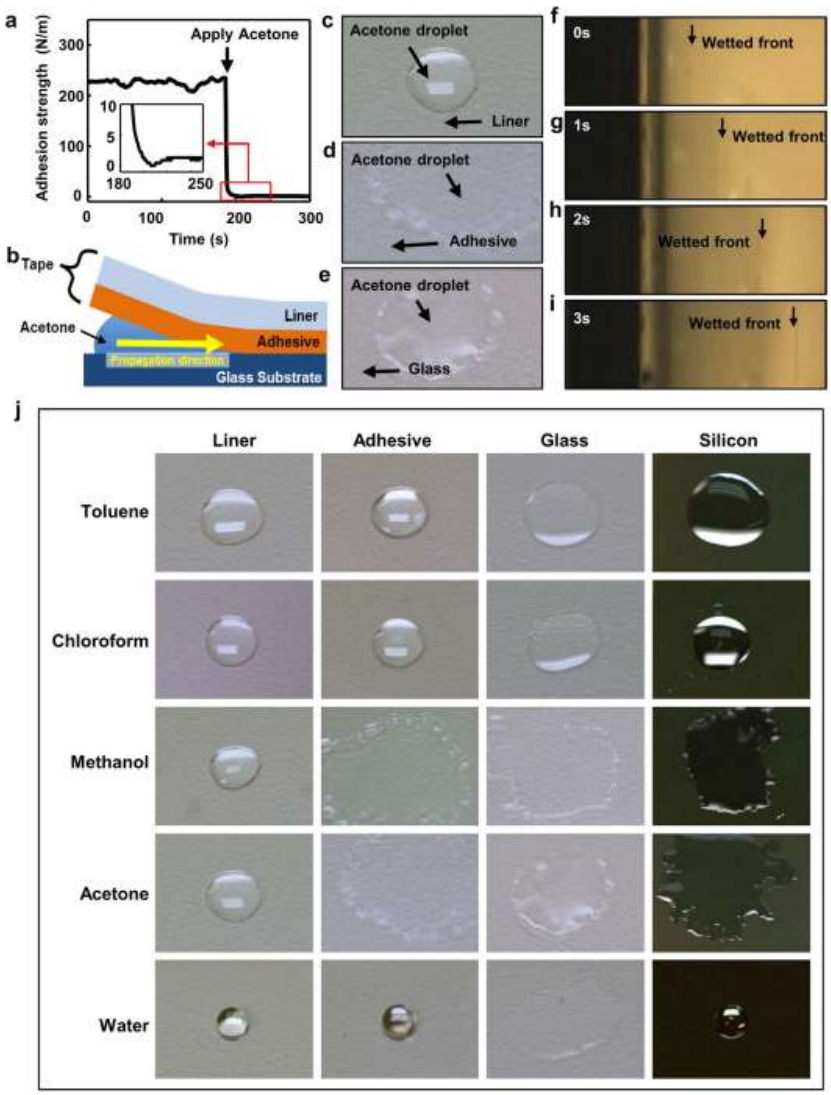

Fig. 14 180° peel test and solvent wetting on substrate test

The recipe for fabrication of silicon dots array on SOI wafer:

1. Dice the SOI wafer into pieces and clean with acetone, IPA and DI water.

2. Prebake at 110℃ for 2min on hotplate for dehydration.

3. Pattern the silicon into square array by photolithography and reactive ion etching (RIE).

4. Immerse the sample into buffer oxide etchant (BOE 1:6) for undercut etching for 15min.

5. Pattern photoresist anchors by photolithography.

6. Immerse the sample into concentrate hydraufluoric acid (HF 49%) for 2hours to remove the SiO_2.

As pointed out, a series of devices can be transfer printed onto flexible substrate to fulfill target functions. Similar to transfer printing of silicon dots array, photodetectors array on polyimide substrate is achievable in the same manner. Figure 15 (a) and (b) show the photodiode array before and after transfer printing. (c) is the microscope blowup of photodiodes on the polyimide film. (d) plots the current-voltage trends of photodiode under illumination and dark environment. The device is proved to be working in the target substrate after transfer printing process.

The recipe for fabrication of photodiode:

1-2. Same as the steps in recipe for fabrication of silicon dots array.

3. Spin coat spin-on-glass (700B Filmtronics) on the wafer and pattern by photolithography and etching to form the doping mask.

4. Phosphorous based spin-on-dopant (P510) was used for doping process at 950℃ to form the diode.

5. Pattern the silicon into square dots array by reactive ion etching (RIE) using sulfur hexafluoride (SF_6) gas.

6-8. Similar to the steps 4-6 in recipe for fabrication of silicon dots array.

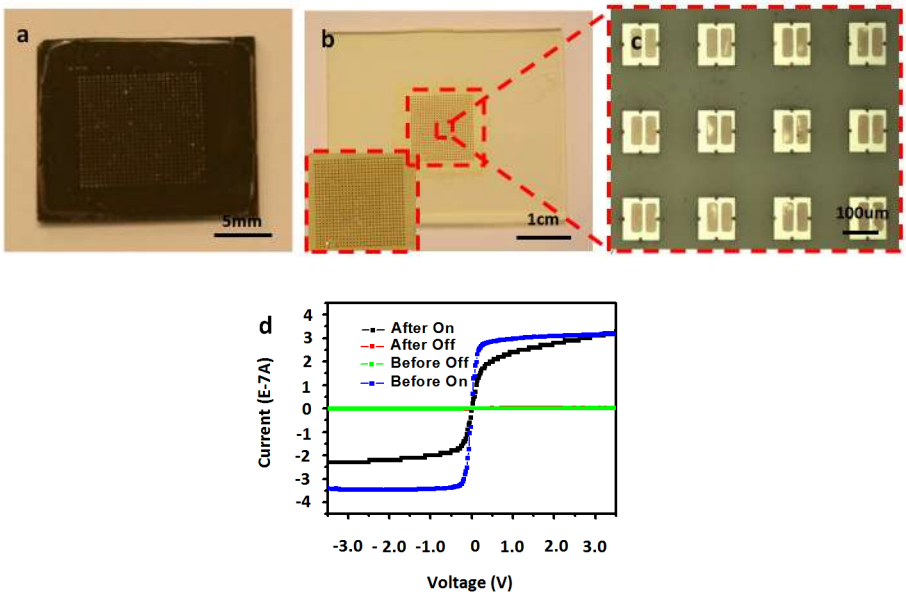

Fig. 15 Tape transfer printing of photodiode array onto Polyimide film

Transfer printing technology is applicable to fabrication of epidermis electronics as it has been reported in the past decade [22, 23, 24]. But tape transfer printing has never been related to any fabrication of e-sensors for physiological monitoring. A kind of skin mountable EMG sensors has been realized based on tape transfer printing and it can work to record EMG signal when being attached on the arm. The sensor was composed of serpentine electrodes and strip pads, which was patterned by photolithography on polyimide-coated glass. The sensor can be transfer printed onto ultralet ozone (O_3) treated Ecoflex patch by tape with assistance of acetone, Figure 16 has shown the flexible EMG sensor and testing. The EMG data acquisition setup was from biomedical engineering department in UH and the testing

program was home-built by MATLAB.

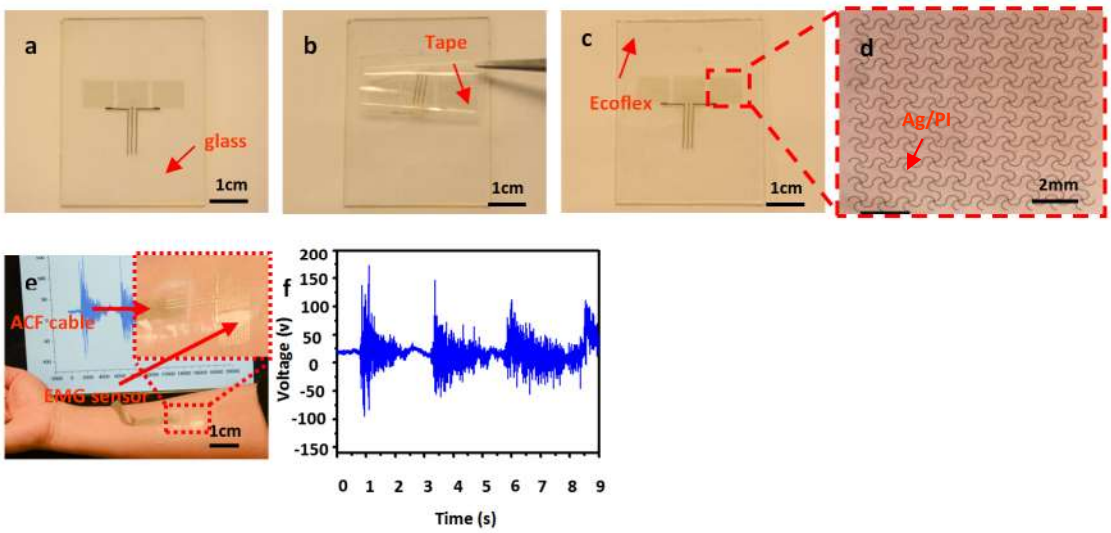

Fig. 16 Transfer printing of EMG sensor onto EcoFLEX patch

The recipe for fabrication of EMG sensor:

1. Clean glass slide with acetone, IPA and DI water, bake it on the hotplate at 110℃ for dehydration.
2. Spin coat polyimide and cure it at 250℃ for one hour.
3. Deposit Ag layer 300nm on the PI by e-beam evaporation.
4. Pattern the electrodes by photolithography.
5. Pattern the PI by RIE under oxygen plasma.
6. Pick up the EMG sensor by using tape 3M3850.
7. Deposit silicon dioxide layer 50 nm on the tape by e-beam evaporation.
8. Spin-coat Ecoflex on the glass and cure at 90℃ for 5 minutes.
9. UV ozone treat the Ecoflex film.

10. Laminate the tape onto the Ecoflex film, heated at 70℃ for 10min to form the bonding between the SiO_2 and the Ecoflex substrate.

11. Prepare acetone in the beaker and immerse the sample in it. Delaminate the tape and leave the electrodes sensor on the Ecoflex film.

12. Bond the ACF ribbon cables between EMG sensor and PCB interface at 170℃ on flat iron for 1min.

13. Peel off the film from glass substrate and connect to the data logger the for testing.

To verify the feasibility of tape transfer printing on other shape substrate, glass tube and glass rod raft were tried as target substrate due to their curvilinear surfaces. Before transfer printing, the tube and glass rod raft was coated with PDMS, Figure 17 shows the silicon dots array printed onto the curvilinear tube and glass rod raft. The diameter of the tube and rod is about 15mm and 5mm respectively.

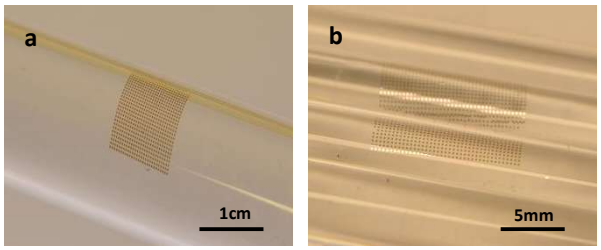

Fig. 17 Transfer printing of silicon dot array onto curvilinear shape tube

Chapter 3

Exploration of fabrication by balloon transfer printing (BTP)

3.1 Introduction

Balloon transfer printing is a novel methodology of fabricating or assembling semiconductor devices onto dome-shape substrate. Generally, the fabrication of dome-shape sensors were started from either transfer print the devices or assemble the devices onto planar substrate, and shape the substrate into curvilinear dome. Google has rolled out a product named smart contact lens that can help monitoring the wearer's glucose level in tear [26]. The fabrication is originated from heat molding technology developed by University of Washington [27], place and press a planar lens with components into a heated aluminum mold to form a curvilinear shape. In this chapter, balloon transfer printing process will be introduced, transfer printing of metal electrodes and silicon square dots array will be demonstrated to verify the possibility of high fidelity. Fabrication of smart contact lens based on balloon transfer printing will be explored, albeit the no functional device is included. And a novel fabrication of hemispherical helix antenna is proposed based on BTP process.

3.2 Smart Contact Lens

Smart contact lenses is coming under the spotlight because of its integrated multi-function features like physiological monitoring and video or image display.

Some companies has already rolled out the commercial product onto the market, specifically Google is taking the lead now and pursuing on making a 'Google glass' like smart contact lens that can realize augmented reality in addition to monitoring the glucose level in tear and the intraocular pressure [27-35]. Also, Samsung has patented smart contact lens that can create augmented reality experience for user [36]. Meanwhile, another consumer electronics giant SONY launched smart contact lenses to capture video and image by blinking eyes [37]. Although numerous categories of smart contact lenses has been created, it is expected that customers will be staggered continuously by more fancy function in the future.

The earliest one of the applications of smart contact lens is used to monitor the glucose level in human body. Today, diabetes is widely considered to be the most deadly disease around the world, and the number of people diagnosed with diabetes mellitus is estimated to increase dramatically in the next few decades, therefore continuous monitoring of glucose can help with diagnosis and prevention of the disease. However, the conventional enzyme-based finger-pricking method used in diabetic assessment is invasive and may cause patient potential infection in the blood sampling process. An alternative method which uses near-infrared spectroscopy opens a door to provide a noninvasive way to infer metabolic concentration by means of analyzing the light reflection or transmission spectrum in the fingertip. Due to the poor signal strength and calibration issues, this method is inappropriate for clinical

use. Therefore, some research institutions and companies are focusing on the sensible development of noninvasive and continuous glucose sensor.

The noninvasive monitoring solution of glucose level proposed by Google is based on electrochemical measurement. The basic electrochemical reaction in sensing glucose is catalyzing glucose to hydrogen peroxide H_2O_2 using the enzyme glucose oxidase (GOD) [38, 39]. H_2O_2 is further oxidized at the electrode to release electrons, generating a current signal proportional to the glucose concentration in the tear. To fabricate a stable electrochemical sensor, three electrodes are typically used: a working electrode (WE) a counter electrode (CE) and a reference electrode (RE). Those comprise the typical electrochemical measurement configuration. Particularly, the working and counter electrodes are designed as concentric rings to decrease the resistance and thus enhance the sensor sensitivity.

The design of the contact lens for glucose monitoring features its circuit implementation, which initially come out of the research in University of Washington. The signal of the on-lens sensor is read out by wireless IC which consists of a power management block, readout circuitry, wireless communication interface, LED driver, and energy storage capacitors in a 0.36mm^2 CMOS chip [39, 40]. The system is wirelessly powered by RF feed from an interrogator, and the energy is converted into stable 1.2-V by rectifier and regulator circuit. The data is transmitted by backscatter communication manner to interrogator to be decoded by the reader. In Google's new

commercial smart contact lens, a compact ASIC chip is used instead of home-built wireless IC to realize the data transmission function.

Besides the application in monitoring the glucose level in tear fluid, other different functions that can make the contact lens smarter has been implemented, such as RF-powered lens with single element display [41]. The micro-LED were grown on an aluminum gallium arsenide, powered by a CMOS chip includes energy harvester, power management unit and energy storage unit. This is a one step forward to realize display of all kinds of text and image in augmented reality style. Afterwards, the researchers have integrated blue micro-LED arrays and micro-Fresnel lenses on the contact lens to create a multi-pixels effect on retina, like letters or numbers or combination of both [42]. It is expected that more than just simple notifications can be given on the lens to have effect of augmented reality. The prototype lens was tried on rabbit's eye and was proven to have a good biocompatibility.

Generally, the power to support smart contact lenses comes from wireless energy transmission. The RF power is fed into the system through antenna from nearby source, but the drawback of this method is the low efficiency of small antenna embedded around the edge of the contact lens and a handheld device is required to send RF wave. To upgrade the energy feed, photovoltaic device like solar cell has been integrated on the contact lens so that it can absorb energy from ambient light and convert it into several microwatts eletrical power, even in-doors [43]. The solar cell

can provide enough energy to make the other devices or chip on lens work. The solar cells were assembled in array and has 14.3% efficiency at AM2.0, it is a little lower than the crystalline solar cell of the near size. But some problems lie in that whether the solar cell can work on the night as well as whether the solar cell would block the vision of the wearer. The feasibility will be unveiled in the future.

Apart from Google, another company focuses on the smart contact lens is the Sensimed Co. The Switzerland located spinoff mainly fabricates patented Triggerfish@ digital active smart contact lens that can continuously monitor wearer's intraocular pressure (IOP) to diagnosis glaucoma, chronic and progressive disease due to the damage of optic nerve that will cause the patient irreversible blindness eventually. The conventional ways to detect the glaucoma is through visual acuity and visual field testing [44], optic nerve examination and tonometry [45], however, those ways are limited and inconvenient because the peak of intraocular pressure occurs on the morning or night, nocturnal measurement of IOP is generally inaccessible. Triggerfish@ can provide 24-hour monitoring of IOP without any interference of wearer's life and sleep, so this helps the doctor identify the best time to measure patient's IOP. So far, the Triggerfish@ has been approved by European regulatory authorities (Class IIa device CE-mark) and available on the market. And FDA has approved the marketing in early 2016.

The key element in Triggerfish@ smart contact lens is a microfabricated

strain gauge that can measure the change in the cornea curvature proportional to the IOP. This technology or method dates back to 1967, when Gillman and Greece presented an embedded strain gauge in contact lens to measure the angular change of corneoscleral junction because of the IOP fluctuation [46]. The drawback of the invention is that the curvature of contact lens has to be the same of that of wearer's eyes. This will make the contact lens expensive and eventually ended up with abandon. Different from strain gauge, the strain gauge used in Triggerfish@ is configured like Wheatstone bridge: two arms act as sensing resistive gauges, and the other two arms act as thermal compensation resistive gauges and placed radically. A dedicated ASIC is used for wireless data transmission at 27MHz, which is a about 50um thick and attached on the lens by common flip-chip technology. This ASIC is connected to a small antenna loop and the active sensor. Energy is fed in from a pair of glasses and a patch for overnight measurement, the data is transmitted onto a portable unit around wearer's waist and sent to PC by Bluetooth.

As a commercial product, Triggerfish@ is proven to have high comfort score during the 24 hour clinical study, a study run on 15 patient attests to the safety and comfort. Despite contact lens malfunction happened on one patient, no other adverse effect was observed. It was reported that non-IOP-related change such as cornea swelling due to the insufficient reach of oxygen through closed eyelid during the wearer's sleep has minimal effect to the data output, hence, the Triggerfish@ smart

contact lens is considered to be a fitting device that can be integrated into the clinical practice and so far it's taking the lead in IOP continuous monitoring device market.

As for smart contact lens for IOP monitoring, researcher H. Cong and T. Pan in UC Davis has developed a contact lens that can real-time measure the IOP [47]. Differ from the resistive pressure gauge embedded in Triggerfish@, such pressure sensor is capacitive sensing features a unique photosensitive composite, which comprises PDMS polymer, silver powder and photosensitive reagent. Pattern a wafer with such composite of photoresist by photolithography and then bond it with flexible substrate, the device is able to be shaped into contact lens by thermal compression. The fabrication is as same as the one used for smart contact lens created by University of Washington, while the planar substrate with devices was pressed in aluminum mold with high temperature, 180℃ to cast a contact lens with desired curvature [48]. However, one of the drawbacks of such a fabrication is the low yield. The devices may easily break in the process of thermal compression; Besides, it is inconvenient to polish the lens edge after molding. Because of this, a better solution is required. A new transfer printing process called balloon transfer printing (BTP) proposed here serves the needs of picking up the devices and transferring to the target contact lens and will reduce the risk of damaging the devices a high yield is expected. Compared to the thermal compression, such technology provides a more sensible option due to convenience and simple operation and will be potentially deployed in fabrication of

smart contact lens in the future. More details about BTP will be covered in the next part.

3.3 Balloon Transfer Printing

The principle of balloon transfer printing process is same to other transfer printing process. Polymer-coated balloon serves as stamp that can be used to pick up the device on the donor and transferred to the receiver. The whole process is illustrated in Figure 18 (a).

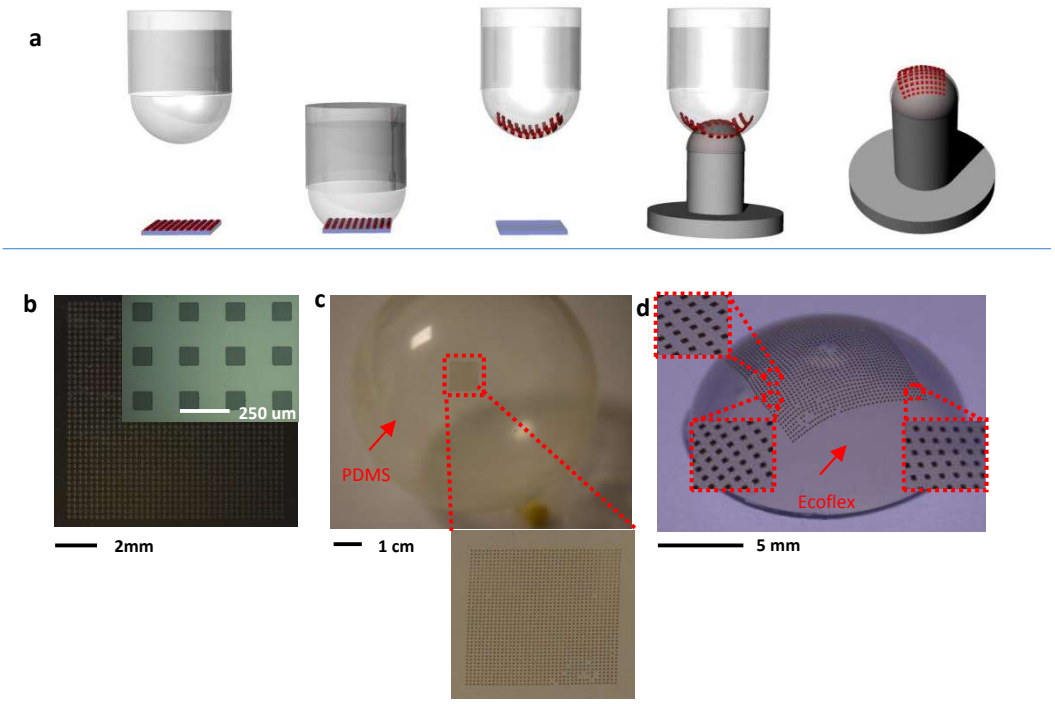

Fig. 18 Balloon transfer printing (BTP) process

250umx250mm silicon square dots array was fabricated following the same recipe as mentioned in last chapter. The balloon was coated by PDMS and left still for 24 hours to dry, then pressed the balloon onto the sample wafer to pick up the dots array,

almost all the silicon pellets can be attached on the PDMS film (Fig. 18 (b)-(c)). The Ecoflex dome was placed on the cylinder stand with hemispherical head after 5-min exposure to UV ozone to strength the bonding. Eventually contacted the balloon onto the dome being heated at 70℃ and retrieved, high fidelity is realized (>99%, Fig. 18 (d)) after the process. One problem in the process is misalignment occurred during the manual operation, but this can be fixed later when PC controlled platform is introduced.

For flexible electronics, all the sensors, chips and electronics components are connected by serpentine interconnects. To verify the metal mesh can be transfer printed by polymer-coated balloon, a copper metal mesh network sandwitched between polyimide film is tested for trial. Fig. 19 (a) and (c) show the 3-layer metal mesh ring, the target dome was moulded and placed on the top of a steel cylinder stand for transfer printing. The final look of the dome with mesh pattern is shown in (b). To verify the feasibility of smart contact lens, some pseudo devices resemble sensors, LED array and contact pads with no function were fabricated in the encapsulation of polyimide films and connected by polyimede serpentine wires to comprise a network. (e) shows a demo of such ‘smart contact lens’ while (d) shows the planar structure before transfer printing. The metal pads were used for connection of ACF ribbon cable for testing. Due to the fact that the sensors have no practical function, no further testing was conducted.

One of applications of balloon transfer printing in fabricating functional device is helix antenna. Conventionally, the hemispherical helix or meanderline antenna is printed onto the conformal substrate like glass by 3D printer [49], directly transfer printed onto contoured substrate [50], or attached on the planar substrate and pneumatically inflated into spherical cap [51]. Similar to the fabrication of devices on hemispherical substrate by BTP, a planar copper antenna is patterned by photolithography first and transfer printed onto the dome, Figure 19 (f) and (g) show the antenna before and after printing. The testing of the antenna was conducted in anechoic chamber, the dome was fixed on the petri dish covered with copper foil and four signal wires were extended from the pads for electrical connection (Figure 19 (h)). Two samples have been tested and result shows a resonant dip at 3.55GHz and 3.52GHz respectively, which matches the simulation result, resonant dip appears at 3.69GHz (Figure 19 (j)).

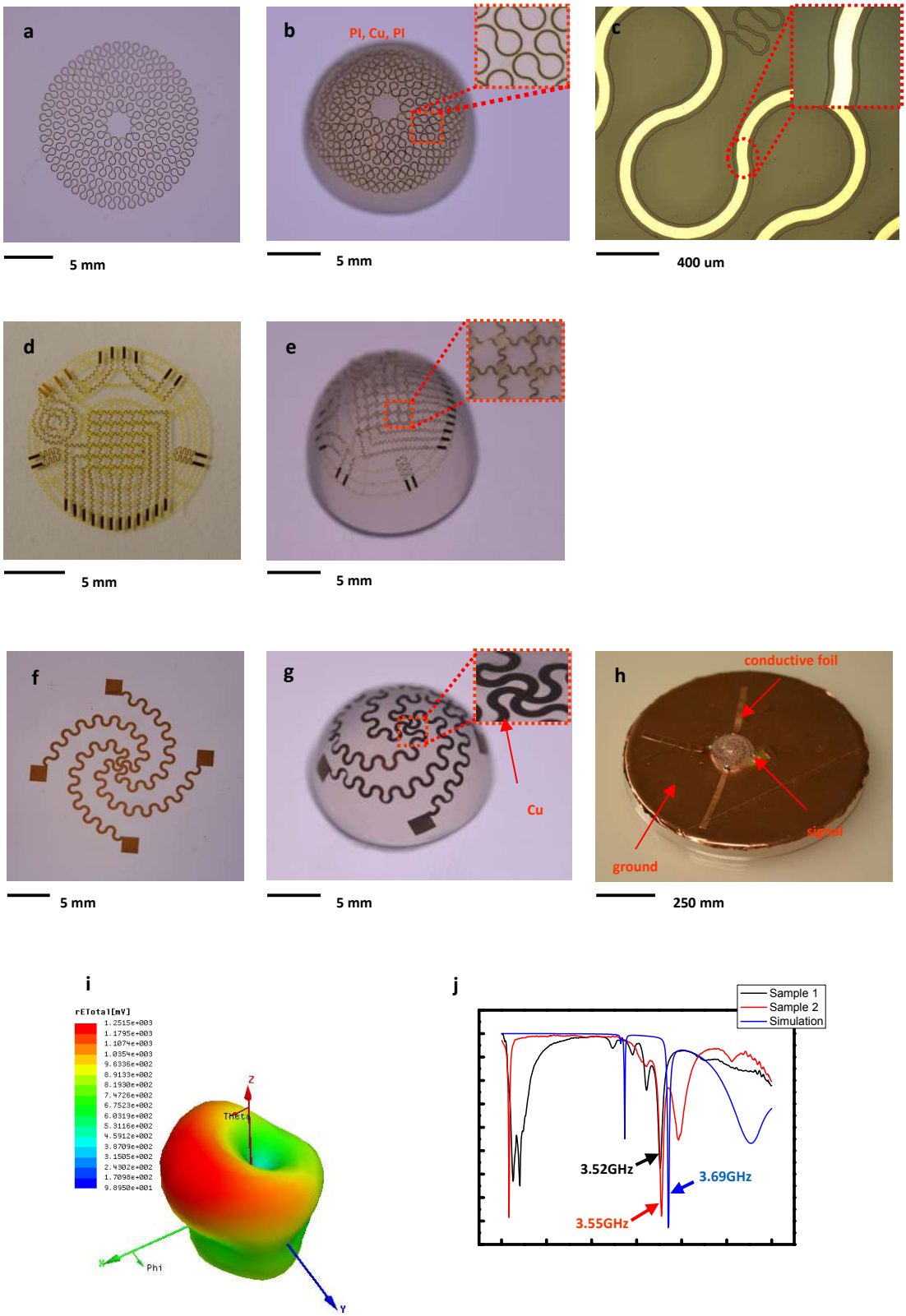

Fig. 19 Transfer printing of serpentine metal mesh and antenna

Chapter 4

Exploration of eSkin technology

4.1 Wearable electronics

‘Wearable electronics are electronic devices constantly worn by a person as unobstructively as clothing to provide intelligent assistance that augments memory, intellect, creativity, communication and physical senses’ [52].

Wearable electronics come under the spotlight in the recent years because they are sensors or computers attached on the human body features compact, flexible and functional. Those devices can be worn in the form of badge, bandage, patch, eyeglasses and wristwatch for the purposes of smart physiological monitoring and all-the-time human machine interaction. Numerous research institutes and companies has put a lot of efforts to develop more sensible and advanced wearable electronics devices. Google has rolled out a pair of glasses that wearer can interact with it to obtain information from internet through natural language voice. Earlier in 2016, Google also developed successfully a smart contact lens that combines multiple functions into the tiny dome. The lens can sense the level of glucose in the tear in eyes and transmit the real-time data to user-end by RF. The is a huge breakthrough because the diabetics don’t need to rely on conventional painful finger-pricking measurement, which requires special device for analysis. And operation at home becomes possible.

Besides Google, Samsung has been working on patented smart contact lens

for augment reality by adding a built-in camera. SONY has synchronously unveiled a contact lens embedded with organic electroluminescence display screen that makes video watching become true, and wearer can control the video recording operation by blinking eyes. To prevent mis-orientation, a gyro is included to detect and bring the video to correct orientation when the user tilts head. Apple doesn't activate their smart contact lens plan but has launched two series Apple Watch incorporated with fitness tracking and health monitoring, seamlessly integrated with iOS. The Apple Watch has built-in sensors include gyroscope, accelerometer and magnetometer as core motion which can track all the wearer's activities, e.g. How much time wearer's spent doing brisk activity and how many calories wearer's burned. And strikingly, ample apps are off the shelf in addition to the activity app on the watch itself, wearer can monitor heart rate if select a health app on the iPhone.

Fig. 20 Google Co.'s Smart Contact Lens for glucose monitoring

4.2 Skin mountable electronics

Courtesy of advances of flexible electronics, a constellation of sensors and

devices become possible to be printed onto the wearer's skin. The so-called 'epidemic electronics' or 'smart bandage' is composed of elastomeric patch, sensors, devices, electronic components and circuit, which can be attached on the surface of epidermis to take measurement of electrophysiological (EP) signal from nerve and muscle activity or other skin properties like temperature, hydration and strain. Usually to acquire EP signal, the electrodes should be laid out in form of serpentine meshes and integrated with skin in conformal manner by Van der Waals interaction. To increase the robustness of measurement, capacitive sensing is employed to encapsulate electrodes between layers of polymer. Figure 21 shows a 3-electrode structure of capacitive sensor and Figure 22 shows comparison of electrocardiograms (ECGs) signal measured by using conventional gel electrodes direct contact (Blue), direct contact electrode (Red), and capacitive epidermis electronics (Green). The conductor is made of metal Au while Solaris is chosen as insulating layer due to its attractive features like large stretchability, adhesion force, strong signal coupling and robust skin lamination. The same capacitive epidermis sensor can also work on electromyograms (EMG) and electrooculograms (EOG) measurement. The EMG signal was recorded on the flexor carpi radialis of the forearm at different motions of hand like in Figure 22 and Figure 23. The EOG signal is measured near left and right eyes when reading a book (Figure 22 (e)). Such epidermis electronics features good wearability and minimum leaking currents, research on combination with wireless

data transmission for telemedicine is being widely conducted.

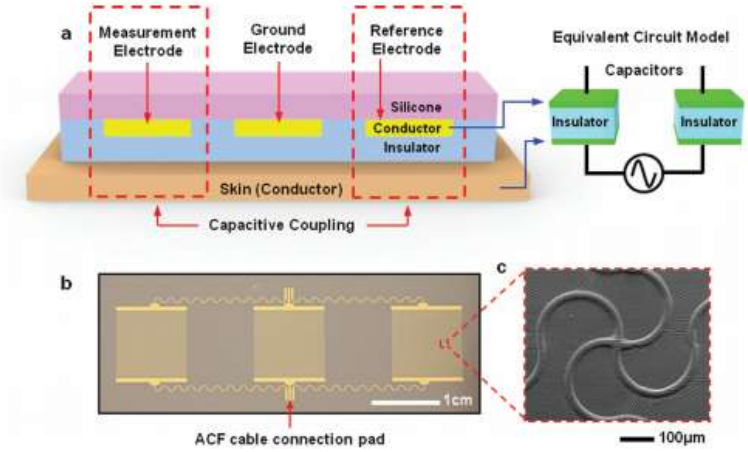

Fig. 21 Capacitive epidermic sensor

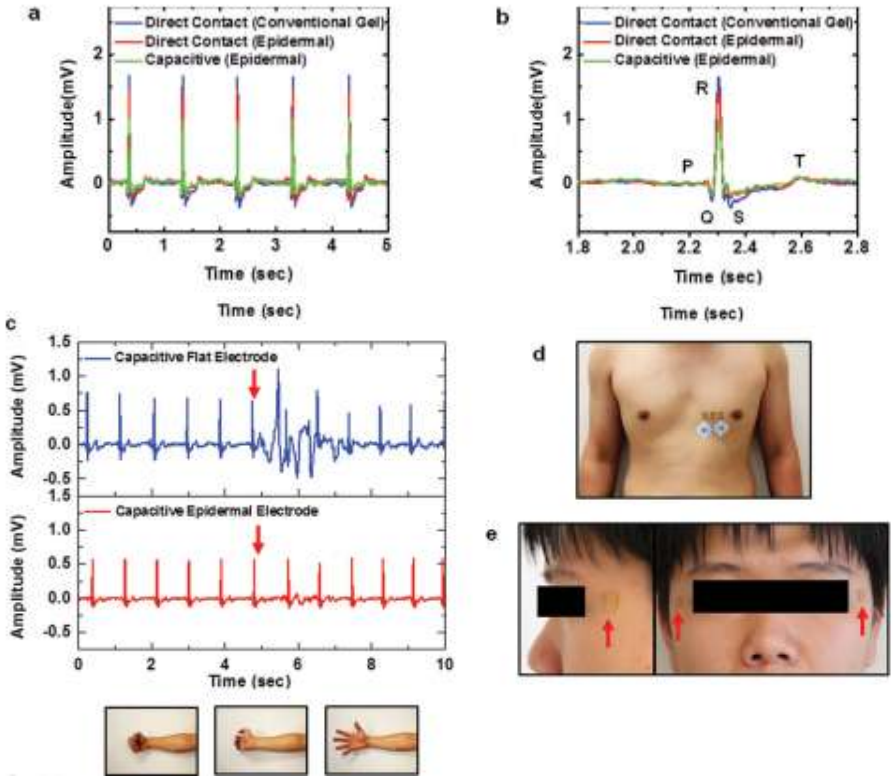

Fig. 22 Electrocardiograms (ECGs) signal and measurement on chest, forearm and near left and right eye

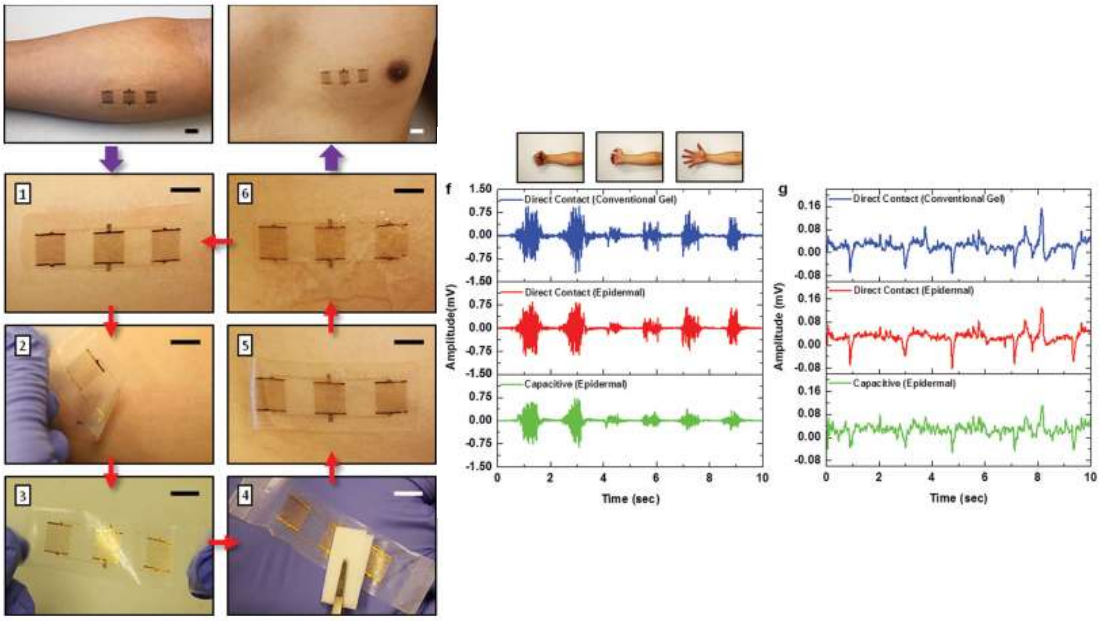

Fig. 23 Electromyograms (EMG) signal measured by capacitive sensor on forearm

4.3 Skin stamps for coupled multi-parametric physiological sensing and environmental monitoring

In this part, a novel skin stamps and multi-sensor monitoring platform will be introduced. Such research is included in a corporate project with WYLE LABORATORIES, NASA Johnson Space Center aims to investigate potential application of flexible electronics on exercise analysis. Some progress about physiological monitoring for astronaut from other institutes will be mentioned in addition to the results generates in the lab in section 4.1. And two methodologies were proposed in the lab: one skin patch encapsulates micro-sensors and devices and the other one encapsulates off-the-shelf sensors for comparison in section 4.2. The testing

for skin patch encapsulates commercial devices will be introduced in section 4.3, an open sourced Arduino Uno platform will be used to log the data acquired from the devices and display the data real-time on GUI by script Section 4.4 demonstrates the experiment results.

4.3.1 Physiological monitoring application for astronauts

To guarantee the safety of astronaut during space flight and extravehicular activities, the physiological condition of the astronaut should be monitored and analyzed real-time. However, unlike people in earth environment, astronaut's body is encapsulated in garment assembly where conventional apparatus and electrical connection is hard to access. To this end, a lot of projects are being sponsored to investigate the applications of biosensors attached on the body that can record the health and psychological data and pass to logging device for processing. NASA and Stanford University aim to develop a system that integrates biosensors and a wearable processing unit called Crew Physiologic Observation Device (CPOD), whose real-time transmission of data to base unit is enabled by Bluetooth wireless technology. Such LifeGuard system is radiation repellent, can survive extreme-rugged environment and integrated function of measurement of blood oxygen saturation, ECG, respiration rate, temperature, heart rate pulse oximetry (SpO2), diastolic and systolic blood pressure. Figure24 shows arrangement of sensors and CPOD straped on the body and details about CPOD.

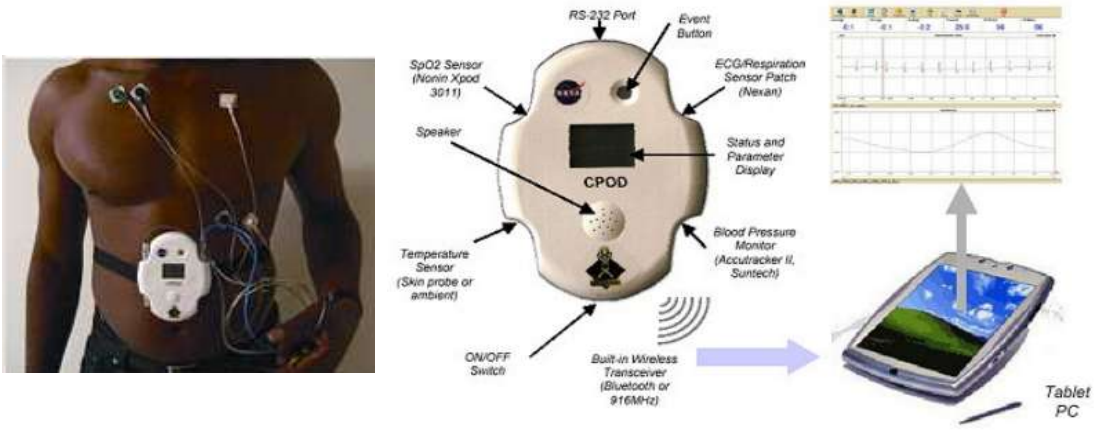

Fig. 24 Crew Physiologic Observation Device (CPOD)

Besides, a Space Sock System composed of heterogenerous sensor network, processor module VPack and spacesuit CAIPack computer was developed by a research group in Virginia Commonwealth University [53], and performance evaluation test was conducted with the supervision of NASA's Extra-Vehicle Activities (EVA) division based in Johnson Space Center. The biomedical sensor signals were acquired by Space Sock that contains plethysmograph sensor, Galvin skin resistance sensor,skin temperature sensor,and a pulse oximetry sensor. The CAIPack in the platform servers as hub for data collection and data presentation on helmet mounted display, and data packets can be routed to remote station in Mission Control Center in Houston. Further development aims to integrate sensors for more physiological monitoring like respiration rate sensor and body accelerator.

Differ from the monitoring sensor network proposed for astronaut's physiological monitoring, a new skin mountable stamps that include various kinds of

sensors in a patch has been developed in Wearable Electronics Group in UH, such stamp can acquire several physiological signals on part of body and send to the processing unit either by wired or wireless communication. More details will be covered in the next part.

4.3.2 Ultra-thin skin mountable stamps

The research on stretchable micro-sensors has been introduced in the previous chapter. It has been demonstrated that the sensors can be transfer printed onto the skin as e-tatoo. Another approach to make a skin stamp is to encapsulate the sensors in elastomer or flexible patch as shown in Figure 25, all the sensors (temerature, UV, strain and ion) are connected in serpentine meshes network. Figure 26 (a) and (b) show the mask design of each seperate sensor, (c) is the blowup that shows the detailed structure. The gold metal layers were sandwitched between polyimide (PI) layers and strikingly, the 6-layer IZO was deposited on the polyimide as transparent electrodes. All the fabrication was carried out in cleanroom in UH and the recipe of fabricating IZO devices is list below:

1. Etch marker (Cu, E-beam & photolithography)
2. Coat Polyimide
3. Coat IZO
4. Pattern IZO (photolithography, wet etching)
5. Deposit 1st metal layer (Au, photolithography & E-beam; lift off)

6. Form gate dielectric (SU-8)

7. Deposit 2nd metal layer (Au, photolithography & E-beam; lift off)

8. Coat Polyimide

9. Pattern PI (photolithography, RIE etching)

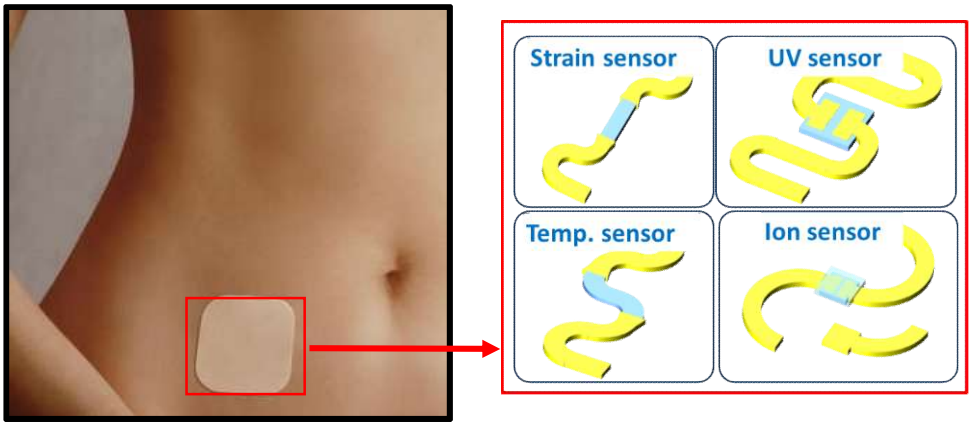

Fig. 25 IZO devices for physiological monitoring

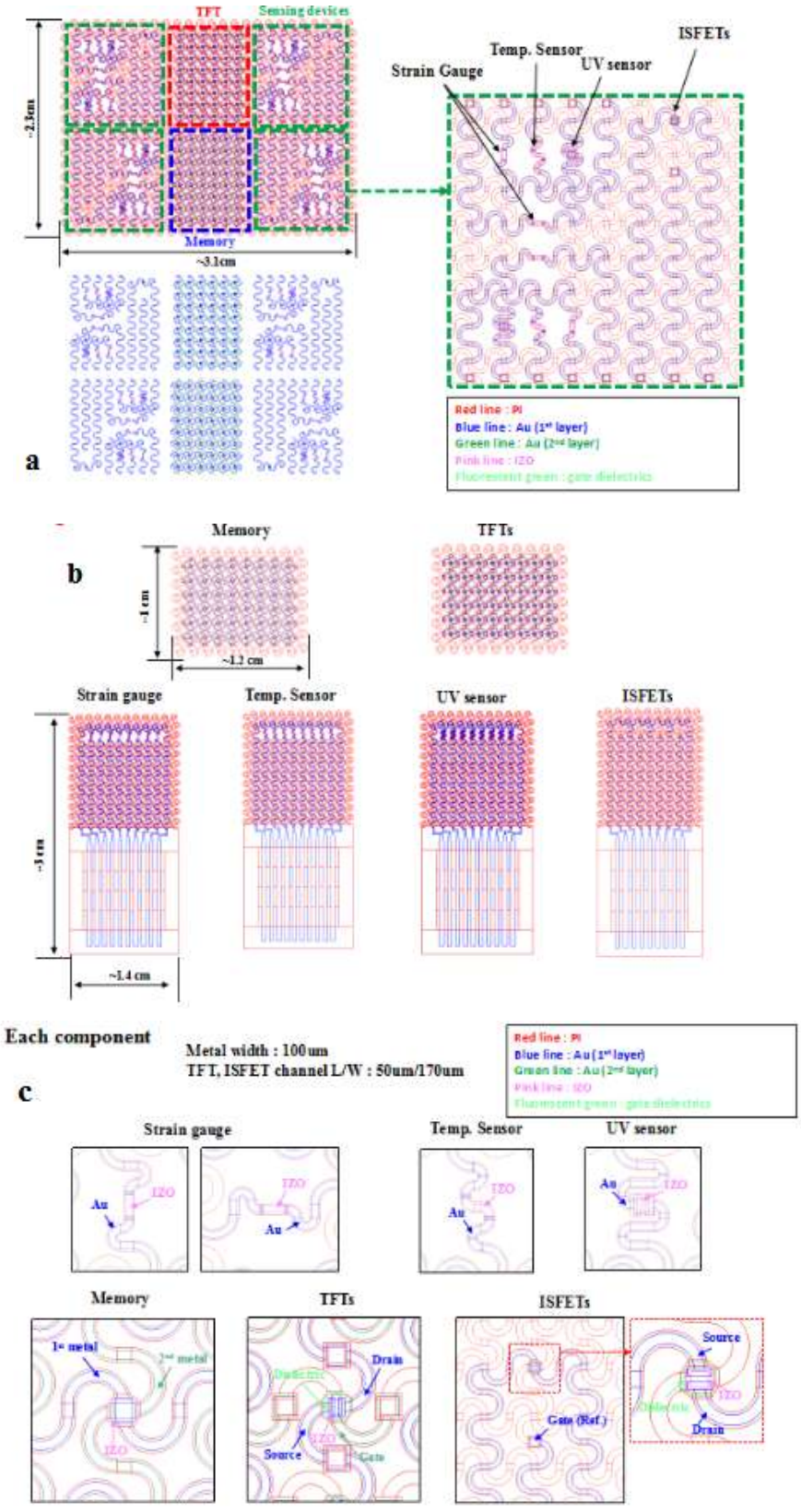

Fig. 26 Mask design of IZO devices

Although the merit of flexibility and delicacy of micro-sensors based skin stamps, the accurate measurement and characterization is difficult while the sensitivity to environment variables seems to be a problem and needs to be decoupled from the measurand. Therefore, some research on skin stamps based on off-the-shelf sensors has been conducted, such epidemic health monitoring system uses interconnected commercial chip and electronic components, one group led by John A. Rogers with university of Urbana-Champaign and Northwestern University has developed such a soft microfludic assemblies that integrates sensors, wireless data transmission, wireless resonant energy coupling and signal conditioning [54]. The interconnects is suspended in fluid that facilitates deformation with little constraint, allows large-range motions with minimal coupling to the system. Figure 27 shows the microfludic assemblies and the its deformation. Figure 28 shows skin patch on forearm for electrophysiological monitoring ((A), (B)) and acquired ECG signal on sternum ((C), (D)).

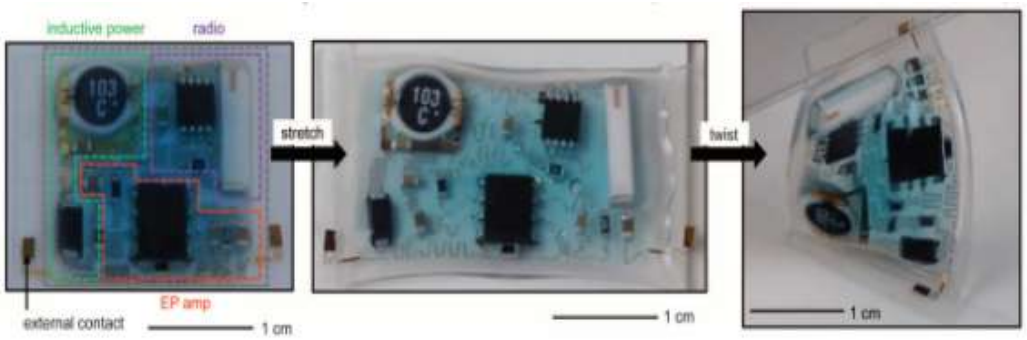

Fig. 27 Microfludic assemblies and its deformation

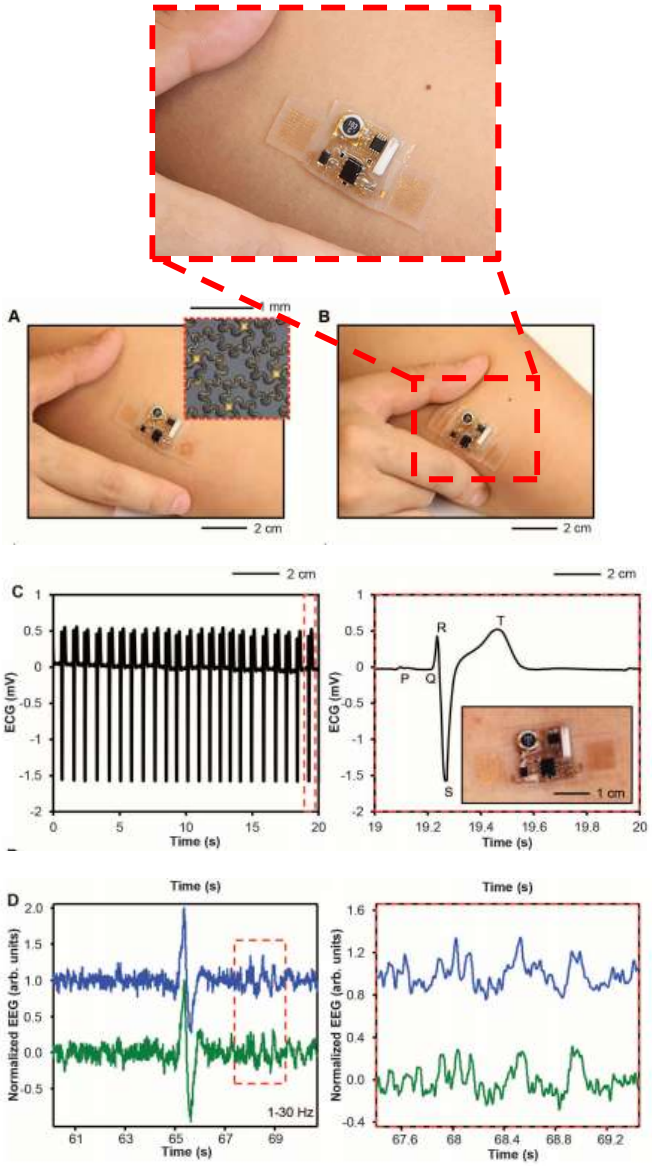

Fig. 28 Skin patch on forearm for electrophysiological monitoring

For the purposes of monitoring multiple physiological parameters of astronaut or athlete, more sensors should be involved besides common temperature, ECG and strain sensors. To this end, one kind of skin patch has been fabricated coupled temperature sensor, skin hydration sensor, pulse rate sensor and gas concentration sensor for exercise analysis. Compared to other skin patch, this skin

patch uses wires transmission in place of wireless data transmission, all the measurand is sent to Arduino Uno development board and displayed on GUI by running a MATLAB script. The schematic of the skin mountable patch is shown in Figure 29.

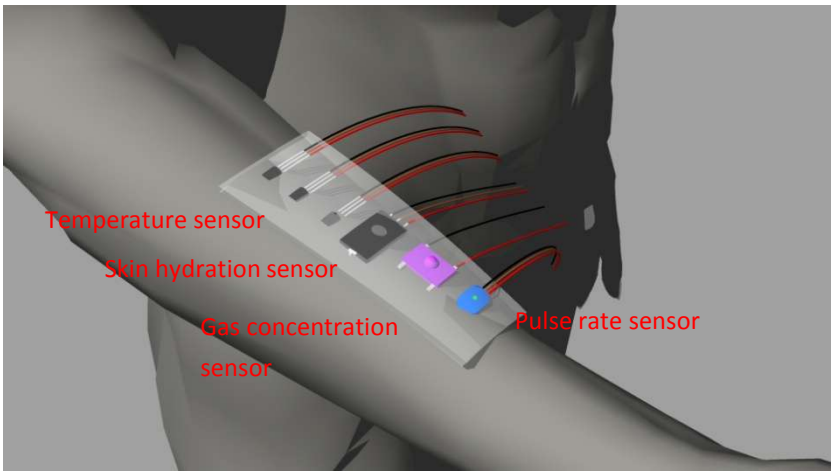

Fig. 29 Skin mountable patch

4.3.2.1 Arduino Uno

Arduino Uno is an open source microcontroller board based on 8-bit AVR RISC-based microcontrollor ATmega328P. It has 14 digital IO ports and 6 analog input ports. The board can be powered either by AC-DC adaptor or USB connection directly. Program in Arduino IDE and download the sketch into the memory can make the board start to work. The whole operation is straight-forward and easy to handle, so it becomes so popular among the electronics geeks and engineers.

4.3.2.2 Sensors

1. Thermistor MCP9700

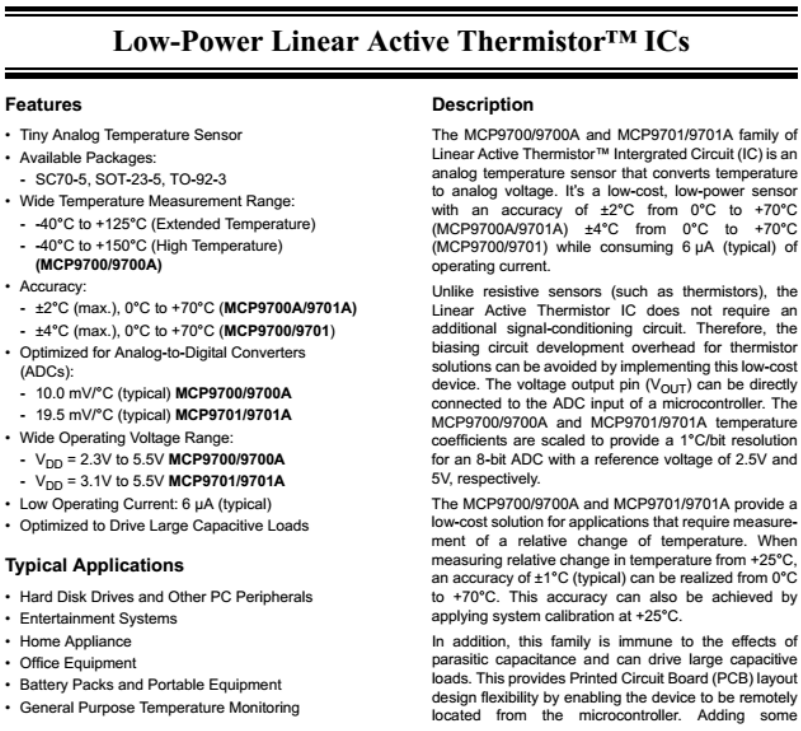

Low-Power Linear Active Thermistor™ ICs

Features

- Tiny Analog Temperature Sensor
- Available Packages:
  - SC70-5, SOT-23-5, TO-92-3
- Wide Temperature Measurement Range:
  - -40°C to +125°C (Extended Temperature)
  - -40°C to +150°C (High Temperature) **(MCP9700/9700A)**
- Accuracy:
  - ±2°C (max.), 0°C to +70°C (**MCP9700A/9701A**)
  - ±4°C (max.), 0°C to +70°C (**MCP9700/9701**)
- Optimized for Analog-to-Digital Converters (ADCs):
  - 10.0 mV/°C (typical) **MCP9700/9700A**
  - 19.5 mV/°C (typical) **MCP9701/9701A**
- Wide Operating Voltage Range:
  - V_{DD} = 2.3V to 5.5V **MCP9700/9700A**
  - V_{DD} = 3.1V to 5.5V **MCP9701/9701A**
- Low Operating Current: 6 µA (typical)
- Optimized to Drive Large Capacitive Loads

Typical Applications

- Hard Disk Drives and Other PC Peripherals
- Entertainment Systems
- Home Appliance
- Office Equipment
- Battery Packs and Portable Equipment
- General Purpose Temperature Monitoring

Description

The MCP9700/9700A and MCP9701/9701A family of Linear Active Thermistor™ Intergrated Circuit (IC) is an analog temperature sensor that converts temperature to analog voltage. It's a low-cost, low-power sensor with an accuracy of ±2°C from 0°C to +70°C (MCP9700A/9701A) ±4°C from 0°C to +70°C (MCP9700/9701) while consuming 6 µA (typical) of operating current.

Unlike resistive sensors (such as thermistors), the Linear Active Thermistor IC does not require an additional signal-conditioning circuit. Therefore, the biasing circuit development overhead for thermistor solutions can be avoided by implementing this low-cost device. The voltage output pin (V_{OUT}) can be directly connected to the ADC input of a microcontroller. The MCP9700/9700A and MCP9701/9701A temperature coefficients are scaled to provide a 1°C/bit resolution for an 8-bit ADC with a reference voltage of 2.5V and 5V, respectively.

The MCP9700/9700A and MCP9701/9701A provide a low-cost solution for applications that require measurement of a relative change of temperature. When measuring relative change in temperature from +25°C, an accuracy of ±1°C (typical) can be realized from 0°C to +70°C. This accuracy can also be achieved by applying system calibration at +25°C.

In addition, this family is immune to the effects of parasitic capacitance and can drive large capacitive loads. This provides Printed Circuit Board (PCB) layout design flexibility by enabling the device to be remotely located from the microcontroller. Adding some

The MCP9700/9700A and MCP9701/9701A family of Linear Active Thermistor Integrated Circuit (IC) is an analog temperature sensor that converts temperature to analog voltage. It is a low-cost, low-power sensor with an accuracy of ±2 ℃ from 0 ℃ to +70 ℃ (MCP9700A/MCP9701A) while consuming 6µA operating current. Strikingly, no signal conditioning circuit is required, the voltage output pin can be directly connected to the ADC input of microcontroller. The temperature coefficients are scaled to provide a 1℃/bit resolution for an 8-bit ADC with a reference voltage of 2.5V and 5.0V respectively.

The connection of temperature sensor and Arduino board is shown below, in

Figure 30. Three wires include power, ground and signal. The signal wire goes into the analog 0 port on the board while the power goes into the +5V port.

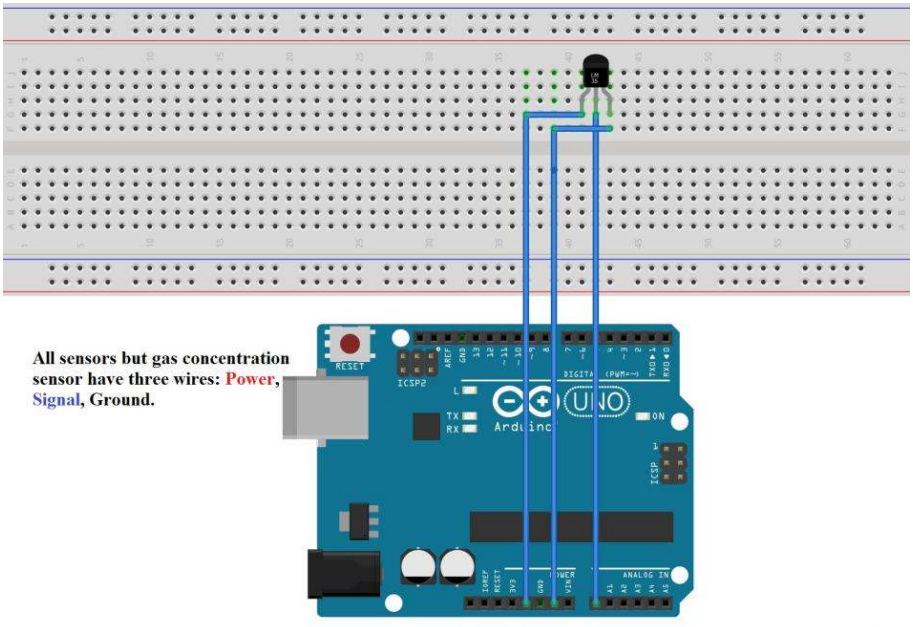

Fig. 30 Thermistor and connection to Arduino Uno

2. Humidity sensor HIH-4030

The HIH-4030/4031 is covered IC humidity sensor that is factory-fitted with a hydrophobic filter allowing it to be used in condensing environments including industrial, medical and commercial application. Direct input to a controller or other device is made possible by the sensor's near linear voltage output. With typical current draw of only 200μA, the HIH-4030/4031 series ideally suited for low drain, battery operated system.

HIH-4030/31 Series

Humidity Sensors

DESCRIPTION

Honeywell has expanded our HIH Series to include an SMD (Surface Mount Device) product line: the new HIH 4030/4031. The HIH 4030/4031 complements our existing line of non-SMD humidity sensors. SMD packaging on tape and reel allows for use in high volume, automated pick and place manufacturing, eliminating lead misalignment to printed circuit board through-hole.

The HIH-4030/4031 Series Humidity Sensors are designed specifically for high volume OEM (Original Equipment Manufacturer) users.

Direct input to a controller or other device is made possible by this sensor's near linear voltage output. With a typical current draw of only 200 µA, the HIH-4030/4031 Series is often ideally suited for low drain, battery operated systems.

Tight sensor interchangeability reduces or eliminates OEM production calibration costs. Individual sensor calibration data is available.

The HIH-4030/4031 Series delivers instrumentation-quality RH (Relative Humidity) sensing performance in a competitively priced, solderable SMD.

The HIH-4030 is a covered integrated circuit humidity sensor. The HIH-4031 is a covered, condensation-resistant, integrated circuit humidity sensor that is factory-fitted with a hydrophobic filter allowing it to be used in condensing environments including industrial, medical and commercial applications.

The RH sensor uses a laser trimmed, thermoset polymer capacitive sensing element with on-chip integrated signal conditioning.

The sensing element's multilayer construction provides excellent resistance to most application hazards such as condensation, dust, dirt, oils and common environmental chemicals.

Sample packs are available. See order guide.

3. Pulse sensor

Pulse sensor ICSG007A is a compact optical pulse sensor that integrates amplification circuit and noise nullification circuit to make pulse readings precise and quick. It consumes 4mA current draw at 5V and can be clipped to earlobe or fingertip for heart rate monitoring when being plugged into the Arduino board.

4. Carbon dioxide sensor

IR1011 from Asahi Kasei Microdevices Corporation feartures world's smallest quantum photodiode (2.65mmX1.9mmX0.4mm), it is SMD package that can be mounted onto PCB of fast response, high sensitivity and no bias current is

required.

It is applicable to human body detection, non-contacting temperature measurement and NDIR gas sensor.

5. Oxygen sensor

No applicable compact oxygen sensor is available after a wide search online, therefore, no oxygen sensor is involved in the demo.

4.3.2.3 Result

To verify the feasibility of skin mountable patch composed of commercial components, temperature and humidity sensors from online shop were chosen and encapsulated into the polymer patch. To this end, EcoFlex rubbers should be prepared by mixing A and B at ratio 1:1 by weight and poured onto the sensor, let alone for couples of hours to solidify. The Figure 31 shows the rubber patch with embedded sensors, and the skin patch attached on the epidermis of arm and data acquisition hardware Arduino Uno board.

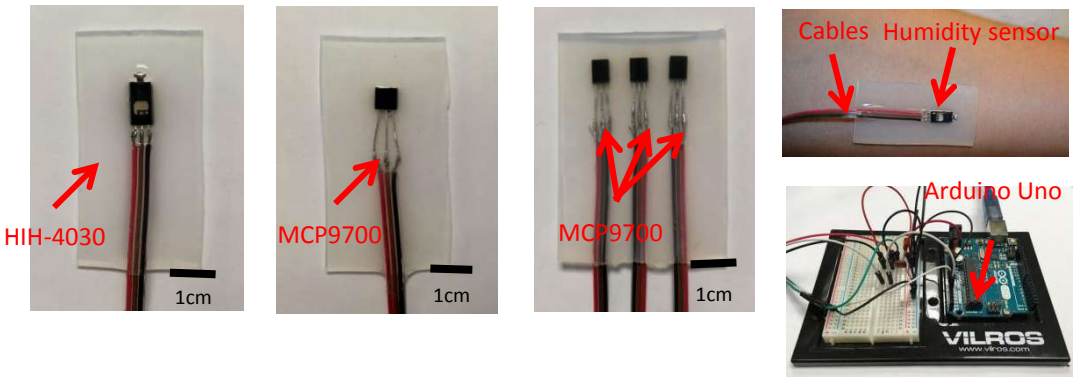

Fig. 31 Skin mountable patch embeds temperature and humidity sensors

The data acquired by the skin patch in 5s is illustrated in the Figure 32 and Figure 33, one is the relative humidity in environment *vs* on skin surface and the other one is the temperature in environment *vs* on skin surface. An evident difference can be found on the on the picture.

RH (%)

Environment	Skin surface
44.06	68.08
43.74	68.24
43.43	68.40
43.43	68.87
43.90	68.24
43.43	68.87
43.59	68.55
43.59	69.03
43.59	68.71
43.90	68.87
43.74	68.55
43.59	68.87
43.74	69.03
43.43	68.87
43.90	68.87

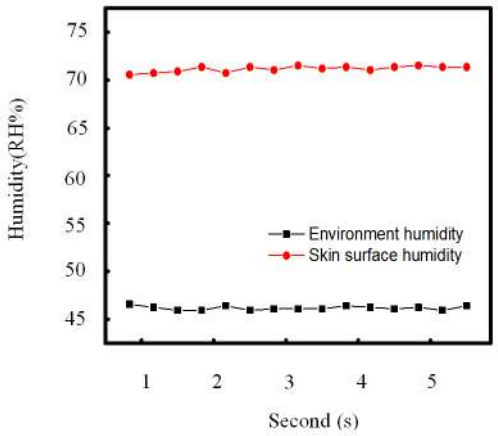

Fig. 32 Humidity in environment and on skin surface

Temperature (℃)

Environment	Skin surface
24.71	31.93
25.00	31.74
24.51	32.13
24.32	32.52
24.32	32.03
24.32	32.13
24.32	32.23
24.51	32.23
24.22	32.32
24.22	32.13
24.22	32.23
24.41	32.03
24.51	32.32
24.22	32.32
24.22	32.52

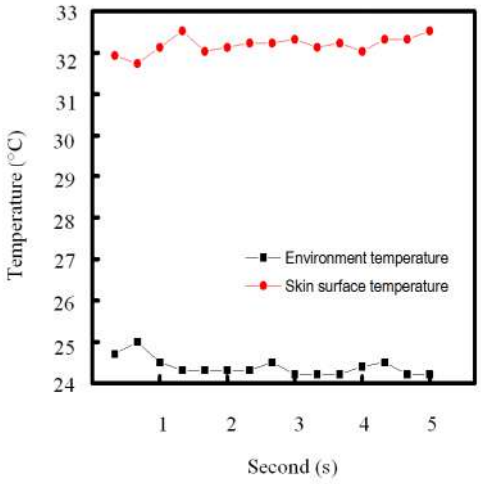

Fig. 33 Temperature in environment and on skin surface

To monitor more physiological signals from astronaut or sportman, more off-the-shelf sensors can be embedded into the Ecoflex patch. Figure 34 shows a skin mountable patch includes pulse sensor and gas sensor besides temperature sensor and humidity sensor. For the purposes of real-time displaying the trend of the acquired signal, a simple script was built by MATLAB, Figure 35 shows the curves of readout. On the right is the data acquisition device and 2-m ribbon cable used for connection to Arduino Uno board. To realize wireless transmission, a transmit-receive module should be deployed and more research can be conducted in the future.

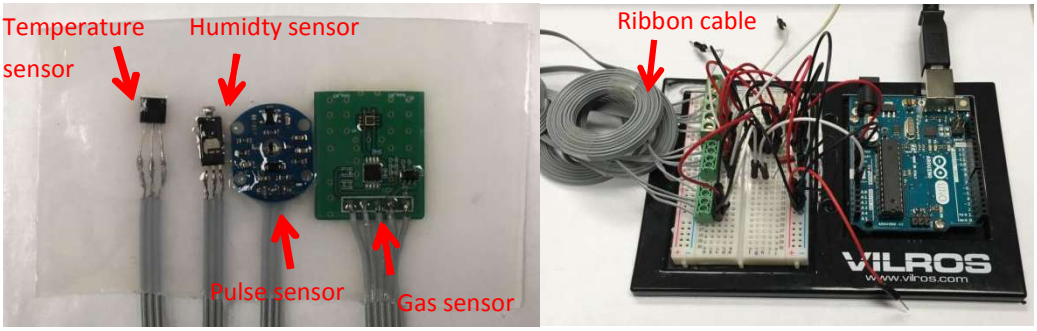

Fig. 34 Skin mountable patch and Arduino Uno

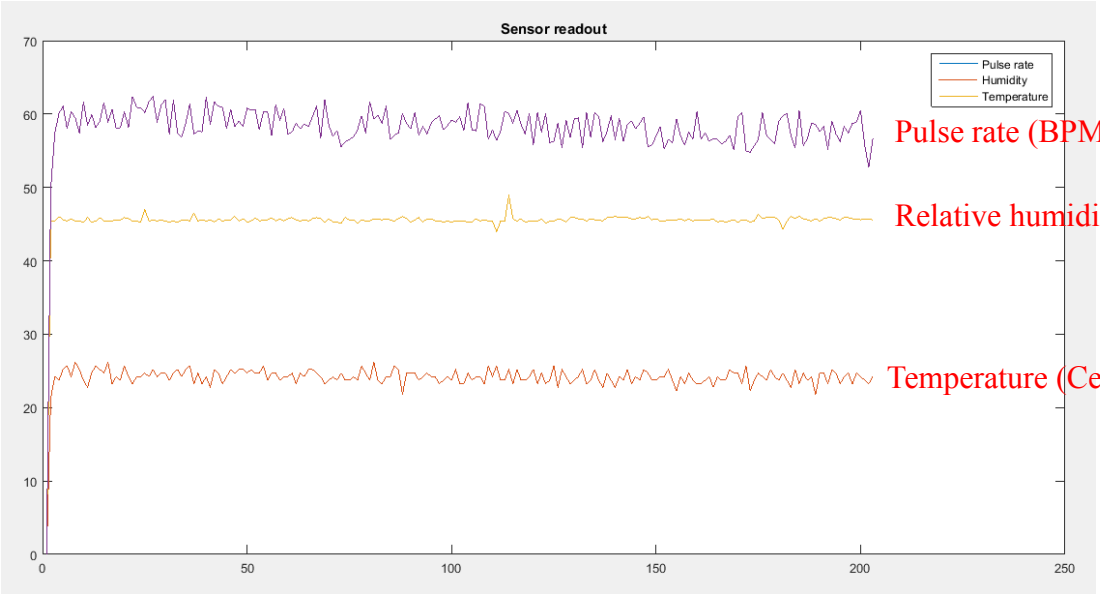

Fig. 35 Real-time acquisition and display of data from sensors

MATLAB script:

```
a = arduino('COM5');

interv = 1000;

passo = 1;

t=1;

x=0;

y=0;

z=0;

while(t<interv)

b=readVoltage(a,'A0');

temp=(b-0.5)/0.01;

x=[x,temp];

fid=fopen('Temperature.txt','w');

fprintf(fid,'Temperature data\n\n');

fprintf(fid,'%f\n',x);

fclose(fid);

c=readVoltage(a,'A1');

RH=161*c/5-25.8;

U=RH/0.9896;

y=[y,U];
```

```
fid=fopen('Humidity.txt','w');

fprintf(fid,'Humidity data\n\n');

fprintf(fid,'%f\n',y);

fclose(fid);

d=readVoltage(a,'A2');

U=d*23;

z=[z,U];

fid=fopen('Pulserate.txt','w');

fprintf(fid,'Pulserate\n\n');

fprintf(fid,'%f\n',z);

fclose(fid);

plot(x);

legend();

grid

t=t+passo;

drawnow;

hold on

plot(y);

drawnow;

hold on
```

```
plot(z);

drawnow;

legend('Pulse rate','Humidity','Temperature');

title('Sensor readout');

end
```

Chapter 5

Conclusion

Introduction to transfer printing especially two novel methods for realization with assistance of tape and coated balloon has been made in this thesis. Experiments on transfer printing of functional devices onto the substrates to form a sensible electronics has been done, especially tentative combination of balloon transfer printing and fabrication of smart contact lens blazes the trail. More research on the balloon transfer is anticipated, heterogenerous integration of multiple devices to consummate smart contact lens will be a good direction although technical hiccups including silicon cracks are subject to effective solution. Besides, research on skin mountable patch for physiological monitoring has been being conducted, in this work, off-the-shelf components and sensors have been tried out to verify the feasibility in real-time application, however, the volume of the devices hinder the attachment onto the skin, therefore more work on design of precise, tiny and applicable flexible devices with convenient communication interface will be conducted in the future.

References

1. Y. N. Xia, J. Tien, D. Qin and G. M. Whitesides, Non-photolithographic methods for fabrication of elastomeric stamps for use in microcontact printing, *Langmuir*, **12**, (1996).

2. J .A. Rogers, J. Tate, W. Li, Z. Bao and A. Dodabalapur, Printed organic transistors and molded plastic lasers, *Israel Journal of Chemistry*, **39**, (1999).

3. J. A. Rogers, Z. Bao, M. Meier, A. Dodobalapur, O. J. A. Schueller, G. M. Whitesides, Printing, molding, and near-field photolithographic methods for patterning organic lasers, smart pixels and simple circuits, *Synthetic Metals*, **115** (2000).

4. A. Kumar and G. M. Whiteside, Features of gold having micrometer to centimeter dimensions can be formed through a combination of stamping with an elastomeric stamp and an alkanethiol "ink" followed by chemical etching, *Appl. Phys. Lett.,* **63 (14)**, (2002).

5. J. L. Wilbur, E. Kim, Y. Xia, G. M. Whitesides, Lithographic molding: A convenient route to structures with sub-micrometer dimensions, *Adv. Mater.* **7 (7)**, (1995).

6. A. Bernald, J. P. Renault, B. Michel and E. Delamarche, Microcontact Printing of Proteins, *Adv. Mater.,* **12 (14)**, (2000).

7. Y.-L. Loo, D. V. Lang, J. A. Rogers, and J. W. P. Hsu, Electrical Contacts to

Molecular Layers by Nanotransfer Printing, *Nano Letters,* **3 (7)**, (2003).

8. Y.-L. Loo, R. L. Willett, K. W. Baldwin and J. A. Rogers, Additive, nanoscale patterning of metal films with a stamp and a surface chemistry mediated transfer process: Applications in plastic electronics, *Appl. Phys. Lett.,* **81 (3)**, (2002).

9. Y. Sun and J. A. Rogers, Printed arrays of aligned GaAs wires for flexible transistors, diodes, and circuits on plastic substrates, Nano. Lett., **4 (10)**, (2004).

10. H. Shimoda, S. J. Oh, H. Z. Geng, R. J. Walker, X. B. Zhang, L. E. McNeil and O. Zhou, Self-assembly of carbon nanotubes, *Adv. Mater.*, **14 (12)**, (2002).

11. J. C. Lewenstein T. P. Burgin, A. Ribayrol, L. A. Nagahara and R. K. Tsui, High-yield selective placement of carbon nanotubes on pre-patterned electrodes, *Nano Lett*., **2 (5)**, (2002).

12. M. A. Meitl, Y. Zhou, A. Gaur, S. Jeon, M. L. Usrey, M. S. Strano and J. A. Rogers, Solution Casting and Transfer Printing Single-Walled Carbon Nanotube Films, *Nano Lett*. **4 (9)**, (2004).

13. S.-H. Hur, O. O. Park, and J. A. Rogers, Extreme bendability of single-walled carbon nanotube networks transferred from high-temperature growth substrates to plastic and their use in thin-film transistors, *Appl. Phys. Lett.*, **86**, (2005).

14. S.-H. Hur, C. Kocabas, A. Gaur, O. O. Park, M. Shim and J. A. Rogers, Printed thin-film transistors and complementary logic gates that use polymer-coated single-walled carbon nanotube networks, *J. Appl. Phys.,* **98**, (2005).

15. H. Ahn, K. J. Lee, A. Shim, J. A. Rogers and R. G. Nuzzo, Additive Soft-Lithographic Patterning of Submicrometer- and Nanometer-Scale Large-Area Resists on Electronic Materials, *Nano Lett.,* **5 (12)**, (2005).

16. M. A. Meitl, Z. -T. Zhu, V. Kumar, K. J. Lee, X. Feng, Y. Y. Huang, I. Adesida, R. G. Nuzzo and J. A. Rogers, Transfer printing by kinetic control of adhesion to an elastomeric stamp, *Nature Materials*, **5**, (2006).

17. E. Menard, Printing semiconductor elements by shear-assisted elastomeric stamp transfer,US 8506867.

18. S. Kim, J. Wu, A. Carlson, S. H. Jin, A. Kovalsky, P. Glass, Z. J. Liu, N. Ahmed, S. L. Elgan, W. Q. Chen, P. M. Ferreira, M. Sitti, Y. G. Huang and J. A. Rogers, Microstructured elastomeric surfaces with reversible adhesion and examples of their use in deterministic assembly by transfer printing, *PNAS*, **107 (40)**, (2010).

19. W. Deng, X. J. Zhang, H. H. Pan, Q. X. Shang, J. C. Wang, X. H. Zhang, X. W. Zhang and J. S. Jie, A High-yield two-step transfer printing method for large-scale fabrication of organic single-crystal devices on arbitrary substrates, *Scientific Reports*, **4**, (2014).

20. S. H. Jeong, K. Hjort, Z. G. Wu, Tape transfer printing of a liquid metal alloy for stretchable RF electronics, *Sensors*, **14 (9)**, (2014).

21. Kyoseung Sim, Song Chen, Yuhang Li, M. Kammoun, Y. Peng, M. W. Xu, Y. Gao, J. Z. Song, Y. C. Zhang, H. Ardebili and C. J. Yu, High fidelity tape transfer printing

based on chemically induced adhesive strength modulation, *Scientific Reports*, **5**, (2015).

22. D.-H. Kim, N. S. Lu, R. Ma, Y. -S. Kim, R. -H. Kim, S. D. Wang, J. Wu, S. M. Won, H. Tao, A. Islam, K. J. Yu, T. -I. Kim, R. Chowdhury, M. Ying, L. Z. Xu, M. Li, H. -J. Chung, H. Y. Keum, M. McCormick, P. Liu, Y. -W. Zhang, F. G. Omenetto, Y. G. Huang, T. Coleman and J. A. Rogers, Epidermal Electronics, *Science*, **12**, (2011).

23. J. H. Kim, A. Banks, Z. Q. Xie, S. Y. Heo, P. Gutruf, J. W. Lee, S. Xu, K. -I. Jang, F. Liu, G. Brown, J. H. Choi, J. H. Kim, X. Feng, Y. G. Huang, U. Paik and J. A. Rogers, Miniaturized Flexible Electronic Systems with Wireless Power and Near-Field Communication Capabilities, *Adv. Func. Mater.,* **25 (30)**, (2015).

24. W.-H. Yeo, Y. -S. Kim, J. W. Lee, A. Ameen, L. Shi, M. Li, S. D. Wang, R. Ma, S. H. Jin, Z. Kang, Y. G. Huang and J. A. Rogers, Multifunctional Epidermal Electronics Printed Directly Onto the Skin, *Adv. Mater.*, **25**, (2013).

25. http://www.newsweek.com/google-patent-cyborg-smart-lens-inject-eyeballs-455824

26. http://www.sammobile.com/2016/04/05/samsung-is-working-on-smart-contact-lenses-patent-filing-reveals/

27. N. M. Farandos, A. K. Yetisen, M. J. Monteiro, C. R. Lowe and S. H. Yun, Contact lens sensors in ocular diagnostics, *Adv. Healthcare Mater.*, **4 (6)**, (2015).

28. Z. H. Liu, Contact lenses having two-electrode electrochemical sensors,

WO2015041716A1, Google Inc., (2015).

29. H. F. Yao, A closed loop control system based on a non-invasive continuous sensor, WO2015076991A1, Google Inc., (2015).

29. J. Etzkorn, Assembling thin silicon chips on a contact lens, US8960899, Google Inc., (2015).

30. Z. H. Liu, Microelectrodes in an ophthalmic electrochemical sensor, US8965478, Google Inc., (2015).

31. J. Etzkorn, B. A. Parviz, Contact lens having an uneven embedded substrate and method of manufacture, US8985763, Google Inc., (2015).

32. J. Etzkorn, Systems and methods for encapsulating electronics in a mountable device, US9009958, Google Inc., (2015).

33. B. Otis, Y. -T. Liao, B. A. Parviz, H. F. Yao, Wireless powered contact lens with glucose sensor, US 20120245444, University of Washington, (2012).

34. J. Pandey, Y. -T. Liao, A. Lingley, R. Mirjalili, B. A. Parviz and B. P. Otis, A fully integrated RF-powered contact lens with a single element display, IEEE Transactions on Biomedical Circuits and Systems, **4 (6)**, (2010).

35. http://mashable.com/2016/04/05/samsung-smart-contact-lenses-patent/#bgZrXUoEYaqO

36. http://www.pocket-lint.com/news/137527-sony-smart-contact-lens-will-record-everything-you-see-with-the-blink-of-an-eye

38. H. Yao, A. J. Shum, M. Cowan, I. Lahdesmaki and B. A. Parviz, A contact lens with embedded sensor for monitoring tear glucose level, *Biosens Bioelectron*, **26(7)**, (2011).

39. Y.-T. Liao, H. F. Yao, A. Lingley, B. A. Parviz and B. P. Otis, A 3 uW CMOS Glucose Sensor for Wireless Contact-Lens Tear Glucose Monitoring, *IEEE Journal of solid-state circuits*, **47 (1)**, (2012).

40. Y.-T. Liao, H. F. Yao, B. A. Parviz and B. P. Otis, A 3 uW wirelessly powered CMOS glucose sensor for an active contact lens, *IEEE International solid-state circuits conference,* (2011).

41. A R Lingley, M. Ali, Y. -T. Liao, R. Mirjalili, M. Klonner, M. Sopanen, S. Suihkonen, T. Shen, B. P. Otis and H. Lipsanen, A single-pixel wireless contact lens display, *J. Micromech./Microengr.,* **21 (12)**, (2011).

42. R. Mirjalili and B. A. Parviz, Microlight-emitting diode with integrated Fresnel zone plate for contact lens embedded display, *J. Micro/Nanolith. MEMS MOEMS*, **11 (3)**, (2012).

43. A. R. Lingley, B. P. Otis, T. T. Shen and B. A. Parviz, A contace lens with integrated micro solar cells, M*icrosystems Technology*, **18 (4)**, (2012).

44. A. S. Hawkins, J. P. Szlyk, Z. Ardickas, K. R. Alexander, J. T. Wilensky, Comparison of Contrast Sensitivity, Visual Acuity, and Humphrey Visual Field Testing in Patients with Glaucoma, *J. Glaucoma*, **12 (2)**, (2003).

45. http://www.healthline.com/health/tonometry#Uses3

46. M. E. Greene and B. G. Gilman, Intraocular pressure measurement with instrumented contact lens, *Invest. Ophthalmol. & Visual Sci.,* **13**, (1974).

47. H. Cong and T. R. Pan, Photopatternable Conductive PDMS Materials for Microfabrication, *Adv. Func. Mater.,* **18 (24)**, (2008).

48. B. P. Otis, Y. -T. Liao, B. A. Parviz and H. F. Yao, Wireless powered contact lens with biosensor, US 8608310, University of Washington, (2013).

49. J. J. Adams, E. B. Duoss, T. F. Malkowski, M. J. Motala, B. Y. Ahn, R. G. Nuzzo, J. T. Bernhard and J. A. Lewis, Conformal Printing of elctrically small Antennas on 3D surfaces, *Adv. Mater.* **23**, (2011).

50. C. Pfeiffer, X. Xu, S. R. Forrest and A. Grbic, Direct Transfer Patterning of Electrically Small Antennas onto Three-Dimensionally Contoured Substrates, *Adv. Mater.*, **24 (9)**, (2012).

51. M. Jobs, K. Hjort, A. Rydberg and Z. G. Wu, A tunable spherical cap microfludic electrically small antenna, *Microfluidic Electronics*, **9 (19)**, (2013).

52. X. Tao, Wearable Electronics and Photonics, *Woodhead Publishing*, (2005).

53. D. -Y. Fei, X. M. Zhao, C. Boanca, E. Hughes, O. Bai, R. Merrell and A. Rafiq, A biomedical sensor system for real-time monitoring of astronauts' physiological parameters during extra-vehicular activities, *Computers in Biology and Medicine*, **40,** (2010).

54. S. Xu, Y. H. Zhang, L. Jia, K. E. Mathewson, K. -I. Jang, J. H. Kim, H. R. Fu, X. Huang, P. Chava, R. H. Wang, S. Bhole, L. Z. Wang, Y. J. Na, Y. Guan, M. Flavin, Z. S. Han, Y. G. Huang and J. A. Rogers, Soft microfluidic assemblies of sensors, circuits and radios for the skin, *Science*, **344 (6179)**, (2014).